Cellular reprogramming with ATOH1, GFI1, and POU4F3 implicate epigenetic changes and cell-cell signaling as obstacles to hair cell regeneration in mature mammals

Amrita A. Iyer[1], Ishwar Hosamani[1], John D. Nguyen[5], Tiantian Cai[2], Sunita Singh[3], Lisa Beyer[4], Hongyuan Zhang[3], Hsin-I Jen[2,3,7], Rizwan Yousaf[3,8], Onur Birol[2,9], Jenny J. Sun[3,10], Russell S. Ray[3], Yehoash Raphael[4], Neil Segil[5,6], Andrew K. Groves[1,2,3] *

[1]Department of Molecular & Human Genetics, Baylor College of Medicine, Houston, TX

[2]Program in Developmental Biology, Baylor College of Medicine, Houston, TX

[3]Department of Neuroscience, Baylor College of Medicine, Houston, TX

[4]Department of Otolaryngology-Head and Neck Surgery, University of Michigan, Ann Arbor, MI

[5]Department of Stem Cell Biology and Regenerative Medicine, Keck School of Medicine of the University of Southern California, Eli and Edythe Broad Center for Regenerative Medicine and Stem Cell Biology at USC, Los Angeles, CA

[6]Caruso Department of Otolaryngology-Head and Neck Surgery, Keck School of Medicine of the University of Southern California, Los Angeles, CA

[7]Current address: Ultragenyx, Cambridge, MA

[8]Current address: NIDCD, Bethesda, MD

[9]Current Address: Georgia Institute of Technology, Atlanta, GA

[10]Current address: Moderna, Cambridge MA

*Corresponding Author: akgroves@bcm.edu

Keywords – Hair cell, Reprogramming, Regeneration, Transcription factor, Inner ear, Cochlear transcriptomics, Hearing loss, Gene therapy

Short Title – Transcription factor reprogramming in the cochlea

ABSTRACT

Reprogramming of the cochlea with hair cell-specific transcription factors such as ATOH1 has been proposed as a potential therapeutic strategy for hearing loss. ATOH1 expression in the developing cochlea can efficiently induce hair cell regeneration but the efficiency of hair cell reprogramming declines rapidly as the cochlea matures. We developed Cre-inducible mice to compare hair cell reprogramming with ATOH1 alone or in combination with two other hair cell transcription factors, GFI1 and POU4F3. In newborn mice, all transcription factor combinations tested produced large numbers of cells with the morphology of hair cells and rudimentary mechanotransduction properties. However, one week later, only a combination of ATOH1, GFI1 and POU4F3 could reprogram non-sensory cells of the cochlea to a hair cell fate, and these new cells were less mature than cells generated by reprogramming one week earlier. We used scRNA-seq and combined scRNA-seq and ATAC-seq to suggest at least two impediments to hair cell reprogramming in older animals. First, hair cell gene loci become less epigenetically accessible in non-sensory cells of the cochlea with increasing age. Second, signaling from hair cells to supporting cells, including Notch signaling, can prevent reprogramming of many supporting cells to hair cells, even with three hair cell transcription factors. Our results shed light on the molecular barriers that must be overcome to promote hair cell regeneration in the adult cochlea.

INTRODUCTION

Hearing loss is a widespread public health issue affecting hundreds of millions of people worldwide. Hearing loss can be treated with cochlear implants or hearing aids but biological restoration of cochlear structure and function is not currently possible. Hearing is mediated by mechanosensitive hair cells in the organ of Corti, and loss or damage to these cells results in sensorineural hearing loss. Although mammals are only capable of very modest spontaneous hair cell regeneration in the balance organs (Bramhall, et al., 2014; Cox, et al., 2014; Golub, et al., 2012; Kawamoto, et al., 2009; Ogata, et al., 1999; Kelley, et al., 1995; Rubel, et al., 1995; Forge, et al., 1993), the cochlea lack this regenerative capability. This is in not the case in lower vertebrates. Robust turnover of hair cells is seen in the balance organs of many non-mammalian vertebrates (Lanford, et al., 1996; Popper and Hoxter, 1990; Jørgensen and Mathiesen, 1988; Corwin, 1981). Impressive structural and functional recovery can also be achieved in the hearing organs of non-mammalian vertebrates following the killing of hair cells (Roberson, et al., 2004; Baird, et al., 2000; Cotanche, 1999; Adler and Raphael, 1996; Roberson, et al., 1996; Niemiec, et al., 1994; Raphael, 1993; Corwin and Cotanche, 1988; Ryals and Rubel, 1988). In these cases, supporting cells lying adjacent to hair cells can re-enter the cell cycle and trans-differentiate to generate new hair cells. These findings have prompted efforts to promote the regeneration of mammalian hair cells through genetic and pharmacological manipulations.

The basic helix-loop-helix transcription factor ATOH1 is both necessary and sufficient for hair cell development and survival (Cai, et al., 2013; Chonko, et al., 2013; Driver, et al., 2013; Pan, et al., 2012; Woods, et al., 2004; Bermingham, 1999). *In vitro* studies using explants of the mammalian cochlea or inner ear balance organs showed that overexpression of ATOH1 can reprogram non-sensory cells of the inner ear into hair cell-like cells (Jen, et al., 2019; Shou, et al., 2003; Zheng and Gao, 2000). Adenoviral expression of *Atoh1* in the cochlea of guinea pigs deafened with ototoxic drugs shows a variable and partial restoration of hearing after the lesion (Izumikawa, et al., 2005). *In vivo* studies employing neonatal transgenic mice showed that cells of the greater epithelial ridge (GER) that lie next to the organ of Corti, and some supporting cells could be reprogrammed to hair cell-like cells with the ectopic expression of *Atoh1* alone (Kelly, et al., 2012; Liu, et al., 2012). However, the hair cell reprogramming ability of ATOH1 declines rapidly with age (Kelly, et al., 2012; Liu, et al., 2012), suggesting a need for additional transcription factors to promote hair cell reprogramming in older

animals. Moreover, cochleae where the auditory epithelium has degenerated further to state lacking hair cell and supporting cells (known as the flat epithelium; (Izumikawa, et al., 2008) do not respond to *Atoh1* over-expression, further indicating the need for a more complex combinatorial approach.

Several transcription factors have been tested in combination with ATOH1 for their hair cell reprogramming potential (reviewed by (Iyer and Groves, 2021). GFI1 and POU4F3 are two hair cell-specific transcription factors expressed downstream of ATOH1 during development that has been implicated in hair cell survival and function (Masuda, et al., 2011; Hertzano, et al., 2004; Wallis, 2003; Xiang, et al., 1998; Xiang, et al., 1997). Adenoviral delivery of ATOH1 and GFI1 to adult mice in which hair cells were ablated promoted regeneration through supporting cell transdifferentiation at a higher efficiency than ATOH1 alone (Lee, et al., 2020). Similarly, transgenic over-expression of combinations of ATOH1, GATA3, and POU4F3 reprogrammed adult supporting cells into hair cell-like cells with improved efficiency (Walters, et al., 2017). A combination of ATOH1, GFI1, and POU4F3 reprogrammed embryonic stem cells and chick otic epithelial cells *in vitro* to cells that expressed several hair cell genes, and showed key hair cell features (Costa, et al., 2015). The co-overexpression of these three factors *in vivo* can also reprogram neonatal Lgr5+ supporting cells into hair cell-like cells more efficiently than ATOH1 alone (Chen, et al., 2021). Finally, the addition of SIX1 to the three factor cocktail was able to reprogram adult mouse tail-tip fibroblasts into hair cell-like cells which have some epigenetic and transcriptional characteristics of hair cells, as well as transduction channel protein expression, and hair cell-like electrophysiological properties (Menendez, et al., 2020).

Recent studies have shown that one reason for the inability of cochlear supporting cells to convert to hair cells is that the chromatin surrounding hair cell genes becomes progressively less accessible as the ear matures (Tao, et al., 2021; Jen, et al., 2019). The use of multiple hair cell transcription factors to reprogram supporting cells into hair cells may enhance the accessibility of hair cell loci in supporting cells, and recent evidence suggests that some hair cell transcription factors such as POU4F3 can do so in the developing cochlea by acting as pioneer factors (Yu, et al., 2021). However, the question of whether combinations of multiple transcription factors simply improve the efficiency of hair cell reprogramming, or whether they can also improve the fidelity of hair cell reprogramming by activating a larger number of hair cell genes is currently unknown.

In this study, we sought to address this question by comparing the reprogramming potential of three transcription factor combinations – ATOH1 alone, ATOH1 + GFI1, and ATOH1 + GFI1 + POU4F3 - in the mouse cochlea. We generated three transgenic mouse lines in which the transcription factor combinations were expressed from the ROSA26 locus in a Cre-dependent fashion. We found that ATOH1 alone is sufficient to reprogram neonatal non-sensory cells of the greater epithelial ridge into a mosaic of large numbers of hair cell-like cells that are surrounded by GLAST-positive supporting cell-like cells. The reprogrammed hair cells resembled inner hair cells and possessed stereocilia and some mechanotransduction properties. At these young ages, additional transcription factors do not enhance the number of new hair cells generated by ATOH1, nor do they increase the number of hair cells genes expressed in these reprogrammed cells, determined by single-cell RNA-seq. However, we show that after the first postnatal week, the overexpression of GFI1 and POU4F3 is necessary to enhance the hair cell reprogramming ability of ATOH1 in 8-day old supporting cells. We also show that some supporting cell populations remain refractory to reprogramming even with three transcription factors, likely due to the action of the reprogramming factors being blocked by Notch signaling delivered by the endogenous hair cells. By simultaneously comparing the transcriptome and chromatin accessibility of cochlear cells at birth and 1 week of age using single cell multi-omic approaches, we showed that hair cell loci become progressively less accessible in supporting cells and non-sensory cells of the cochlea during the first postnatal week. Our work provides the first mechanistic analysis of hair cell reprogramming and reveals some of the epigenetic and cell signaling obstacles that will need to be overcome in a therapeutic context in the mature inner ear.

RESULTS

Hair cell transcription factors promote highly efficient reprogramming of non-sensory cochlear tissue into hair cell-like cells in the neonatal mouse

To directly compare the efficiency of different transcription factor combinations in hair cell reprogramming, we targeted them to the *Rosa26* locus using a modified *Ai3* targeting vector containing a transcriptional stop cassette flanked by loxP sites (Madisen, et al., 2010). We used three different hair cell transcription factor combinations: ATOH1 alone, GFI1 & ATOH1, and GFI1, ATOH1 & POU4F3 (Figure 1A). Individual transcription factor coding regions were separated by a GSG-T2A self-cleaving peptide sequence to ensure comparable transcription factor expression levels (Tang, et al., 2009). We were able to achieve correct targeting efficiency to the *Rosa26* locus of approximately 80% by co-electroporating our targeting vectors with a plasmid expressing Cas9 and a sgRNA targeting the *Rosa26* locus between the two homology arms. This high efficiency allowed us to obtain correctly targeted ES cell clones with multiple constructs in single electroporation. We verified the expression of the transcription factor proteins by culturing the mouse ES cell lines used to generate founders for the three targeted mouse lines in the presence of membrane-permeable TAT-Cre protein, followed by western blotting (Figure 1 – Supplementary Figure 1A).

We targeted overexpression of the three-hair cell transcription factor combinations to the greater epithelial ridge (GER) and supporting cells of the neonatal mouse organ of Corti using *Sox9-CreER* transgenic mice (Figure 1B; (Kopp, et al., 2011). We confirmed GER and supporting cell-specific targeting with this mouse line by administering tamoxifen to one-day-old (P1) *Sox9-CreER; RosaEGFP* (Ai3) mice and analyzing their cochleae a week later (P8; Figure 1C). The pattern of recombination in GER cells and apical turn supporting cells corresponded to the normal expression of SOX9 protein at this age, revealed by EGFP expression and the absence of recombination in hair cells (Figure 1 – Supplementary Figure 1B). All three *Rosa26*-targeted mouse lines were bred with *Sox9-CreER* to obtain experimental mice harboring both alleles. For the remainder of the manuscript, we will refer to mice carrying the *Sox9-CreER* allele and the *Rosa26*-targeted transcription factor combinations as Rosa-A, Rosa-GA, and Rosa-GAP (Figure 1B). We activated each combination of transcription factors in the GER and supporting cells by injecting tamoxifen at P1 and analyzing mice one week later.

We immunostained the 8-day-old reprogrammed cochleae for the hair cell marker Myosin VIIA and the presence of actin-rich hair bundles with fluorescently-labeled phalloidin. We observed efficient reprogramming of GER cells into hair cell-like cells (Figure 1D), with large numbers of reprogrammed Myosin VIIA+/phalloidin+ cells throughout the GER, extending from the neural edge of the organ of Corti to the interdental cell region (Figure 1D). These ectopic cells could survive in the GER until at least 15 days after birth (Figure 1 – Supplementary Figure 2). Reprogrammed hair cells were present in similar numbers throughout the basal-apical axis of the cochlea, with an average of 300 reprogrammed hair cells per 200μm, compared to an average of 28 inner hair cells and 90 outer hair cells in a corresponding 200μm length of the organ of Corti. We did not observe significant differences in reprogrammed hair cell numbers between the three transcription factor combinations at this age (Figure 1E). We characterized the P8 reprogrammed hair cell-like cells by immunostaining for known hair cell and supporting cell markers (Figure 2A). The reprogrammed cells in the GER expressed VGLUT3, a known vesicular transport protein expressed in inner hair cells (Obholzer, et al., 2008; Ruel, et al., 2008) (Figure 2A). The reprogrammed cells did not express Prestin, a motor protein specific to outer hair cells which is necessary for their electromotility and their contribution to cochlear amplification and tuning (Zheng, et al., 2000). The reprogrammed hair cell-like cells in the GER received innervation from auditory afferents, labeled with the TuJ1 antibody to βIII-tubulin. The hair cell-like cells also stained with antibodies to the CTBP2 transcription factor, which also recognizes Ribeye, a major component of ribbon synapses formed between afferent neurons and hair cells (Sheets, et al., 2011).

To further characterize the hair cell-like cells, we used scanning electron microscopy to assess the morphology of reprogrammed hair cell stereocilia and compared it to that of endogenous hair cells. Under all three reprogramming conditions, reprogrammed hair cells throughout the GER had stereocilia-like protrusions from their apical surfaces, possessing a staircase-like arrangement of hair bundles that appeared similar to control hair cells of the same age (Figure 2B). To determine the presence of mechanotransduction channel activity, we incubated explants of our P8 cochleae with the styryl dye FM 1-43, which permeates transduction channels. Hair cells mature in a basal-apical gradient along the cochlear duct, and between P6 and P7, all hair cells in the cochlea have matured to the point where they are permeable to FM1-43 dye (Lelli, et al., 2009). Reprogrammed hair cells in the GER in all three conditions took up the FM 1-43 dye within 10 seconds (Figure 2B), although the degree of labeling of the reprogrammed cells in the GER was significantly fainter than the

endogenous hair cells visible in the organ of Corti. In sum, we established that under all three combinations of hair cell transcription factors, we generated large numbers of reprogrammed inner hair cell-like cells that are innervated, are morphologically similar to endogenous hair cells, show ribbon synapse formation, and possess some mechanotransduction channel activity.

To test if cell proliferation played a role in the generation of the reprogrammed hair cells in the GER, we assayed cell proliferation in the reprogrammed cochleae using EdU incorporation. Experimental and control animals were injected with tamoxifen at P1 to initiate transcription factor overexpression, followed by EdU injections (50mg/kg body weight) twice every other day until P8. We observed that cell proliferation occurred only in the spiral ganglion region and not in the organ of Corti of experimental or control animals, and none of the reprogrammed hair cells in the GER were labeled by EdU (Figure 2 – Supplementary Figure 1). These data suggest that the vast majority of the reprogrammed hair cells we observe in the GER are generated by direct non-mitotic reprogramming, rather than by proliferation.

scRNA-seq analysis reveals that cochlear reprogramming in newborn mice generates new hair cells that are similar to their endogenous counterparts

Our data suggested that the gross phenotype of the reprogrammed hair cell-like in neonatal mice resembled wild type hair cells, and did not vary significantly between the three reprogramming conditions. To determine whether unique transcriptional changes occurred in response to the three reprogramming conditions, we performed single-cell RNA-sequencing analysis of the reprogrammed cells. We bred the *Sox9-CreER* mice to the Ai9 *Rosa-tdTomato* reporter line and further bred these to the three Rosa26 conditional overexpression lines (Figure 3A) to obtain our experimental mice, where one ROSA26 allele carried a tdTomato reporter, and the other ROSA26 allele carried one of the three reprogramming cassettes. These mice were injected with tamoxifen at P1 and tdTomato-positive cochlear cells were purified by FACS at P8 (Figure 3A) and used to generate scRNA-seq libraries using the 10xGenomics Chromium platform.

The cell clustering pattern observed after the integration of cells from all four genotypes allowed us to identify expected cell-type-specific clusters based on transcriptomic data from previous studies (Kolla, et al., 2020). Sensory and non-sensory cells of the cochlear duct, including hair cells, supporting cells, greater epithelial ridge cells, cells of the stria vascularis, and glial cells were all identified in the clustering (Figure 3B).

Examples of marker genes used to validate cluster identification on the basis of their expression in the hair cell and lateral GER clusters is shown in Figure 3 – Supplementary Figure 1. Our clustering analysis confirmed the results obtained by staining with cell type-specific markers: we saw a reduction in cells of the GER (particularly lateral GER) but a significant increase in the numbers of hair cells in the three reprogrammed conditions compared to control mice (Figure 3C). Other cochlear cell types that were identified during this analysis are indicated in the diagram in Figure 3D. We performed a gene ontology analysis (GO- Biological process) to ascertain the morphological and functional characteristics of these reprogrammed hair cells. We identified 496 genes significantly expressed genes in the reprogrammed hair cells across all three overexpression conditions (cut off p-value < $1.00E^{-25}$) which were used as input for gene ontology analysis. The top GO hits included genes for sensory perception of sound (GO: 0007605, 27 genes, $p=1.40E^{-13}$), inner ear morphogenesis (GO: 0042472, 12 genes, $p=5.70E^{-04}$), auditory receptor cell differentiation (GO: 0042491, 7 genes, $p=5.70E^{-04}$), cilium morphogenesis (GO:0060271,17 genes, $p=7.50E^{-04}$) and cell projection organization (GO:0030030,16 genes, $p=7.50E^{-04}$; Figure 3E). Together, our data suggest that reprogrammed hair cells possess many morphological and transcriptional characteristics similar to endogenous inner hair cells. However, they also show that at this age, the addition of Gfi1 and Pou4f3 does not improve the morphology of the reprogrammed hair cells, nor a more complete complement of hair cell genes expressed in the reprogrammed cells.

Overexpression of GFI1 and POU4F3 enhances the hair cell reprogramming ability of ATOH1 in the mouse cochlea at older ages

Our data show that all three transcription factor combinations have similar hair cell reprogramming potential in the neonatal mouse cochlea. Previous overexpression studies have shown that the reprogramming efficiency of ATOH1 declines with increasing age (Kelly, et al., 2012; Liu, et al., 2012). We next explored the *in vivo* reprogramming potential of our transcription factor combinations in older animals. Employing the same experimental mouse breeding scheme as described above, we overexpressed the three transcription factor combinations (ATOH1, GFI1 & ATOH1 and GFI1, ATOH1 & POU4F3) in the GER and organ of Corti, including all supporting cells, again using *Sox9-CreER* mice (Figure 4A). We confirmed correct and efficient recombination in GER and supporting cells by administering tamoxifen in one week old (P8) *Sox9-CreER; RosaEGFP* mice and analyzing GFP reporter expression by immunostaining a week later (P15; Figure 4B).

Between P7 and P15, parts of the GER undergo remodeling through thyroid hormone-dependent apoptosis and are replaced by cuboidal inner sulcus cells (Peeters et al., 2015). By P15 several rows of SOX9+ GER cells remain on the lateral edge of the inner sulcus adjacent to the organ of Corti. These are still targeted correctly by *Sox9-CreER* mice (Figure 4 – Supplementary Figure 1A).

We compared overexpression of the three transcription factor combinations by giving tamoxifen at P8 to Rosa-A, Rosa-GA, and Rosa-GAP mice harboring the *Sox9-CreER* allele to target the GER and supporting cells. Analysis of the mice a week later (P15) with the hair cell markers Myosin VIIA and phalloidin revealed that reprogrammed hair cells were significantly higher in the Rosa-GAP condition (average GAP reprogrammed hair cells – 55, Inner hair cells- 31, Outer hair cells – 95 per 200μm length of the organ of Corti; Figure 4D). These new hair cells continued to survive until at least P29 and showed increasing organization of phalloidin-stained hair bundles with increasing age (Figure 4 – Supplementary Figure 1B). Immunostaining of the reprogrammed cells revealed that, unlike the younger reprogrammed cells, P15 reprogrammed hair cells in the Rosa26-GAP condition did not express the inner hair cell marker VGLUT3 (Figure 5A). These reprogrammed hair cells did, however, show evidence of innervation based on staining with TuJ1 antibody, and formed ribbon synapses based on positive staining for CTBP2 (Figure 5A). We used scanning electron microscopy (SEM) to assess the morphology of reprogrammed hair cell stereocilia across all three conditions. Low power images showed the presence of sparse reprogrammed hair cells in the ATOH1 and GFI1+ATOH1 overexpression conditions which did not stain for any hair cell markers other than Myosin VIIA (Figure 5B). Higher magnification SEM images at 50,000X revealed that individual hair cell stereocilia of reprogrammed hair cells in all three conditions were immature compared to endogenous hair cells and the P1 reprogrammed hair cells we observed at P8. Many of the ectopic cells possessed kinocilia but the stereocilia did not exhibit a staircase-like structure and still contained many side links between individual stereocilia, indicating their immature state (Figure 5B). Together, we established that all three overexpression conditions are capable of producing reprogrammed hair cell-like cells at P15, but the Rosa26-GAP cocktail is significantly more efficient at producing new hair cells. Nevertheless, these reprogrammed hair cells created between P8 and P15 are less mature than those derived from reprogramming neonatal cells between P1 and P8..

To determine whether the hair cells generated by overexpression of ATOH1, GFI1, and POU4F3 expressed more elements of the hair cell gene regulatory network, we repeated the scRNA-seq analysis described above on our three mouse lines, applying tamoxifen at day 8 and sorting and analyzing cells at P15 (Figure 6A). The genotype-integrated cell clustering pattern obtained allowed us to identify expected cell-type-specific clusters based on marker expression data from prior studies (Ranum, et al., 2019). We identified multiple cell types in the clustering, including glial cells, hair cells, supporting cells, cells of the stria vascularis, spiral limbus, and interdental cells (Figure 6B). Examples of marker genes used to validate cluster identification on the basis of their expression in the hair cell and supporting cell clusters is shown in Figure 6 – Supplementary Figure 1. Initial clustering analysis confirmed our earlier findings that the number of reprogrammed hair cells obtained in response to overexpression of GAP factors is greater than the small number of hair cells seen with GFI1 + ATOH1 or ATOH1 alone (Figure 6C). Other cochlear cell types identified in the analysis are indicated in the organ of Corti diagram using identical color coding to the UMAP plots (Figure 6D).

To elucidate the characteristics of the reprogrammed hair cells, we identified a list of 200 significantly expressed genes in hair cells obtained from each of the three overexpression conditions (cut off p-value < $1.00E^{-15}$). We performed a gene ontology analysis to ascertain the overall characteristics of these reprogrammed hair cells and look for possible differences (Figure 6E). The top GO terms included genes for cell projection (GO:0042995), cytoskeleton (GO:0005856), cilium (GO:0005929) - Cellular component, Cell projection organization (GO: 0030030) - Biological process, calcium ion binding (GO: 0005509), calmodulin-binding (GO: 0005516) - Molecular function. Taken together, we have shown that hair cells obtained from all three overexpression conditions are transcriptionally similar and possess immature hair cell-like features. However, although the Rosa26-GAP reprogramming mice generate more hair cells, their transcriptional profile did not differ significantly from hair cells observed in ROSA-A or ROSA-GA conditions, suggesting that the additional reprogramming factors increase the efficiency, but not the fidelity of hair cell reprogramming.

Hair cell reprogramming of the greater epithelial ridge generates a mosaic of hair cells and supporting cells through activation of Notch signaling

A consistent observation in our reprogramming experiments conducted between P1-P8 and P8-P15 was that some supporting cells of the organ of Corti – the Deiters' cells and pillar cells – did not respond to the reprogramming factors by expressing hair cell proteins such as Myosin VIIA and did not exhibit any morphological changes indicating they were transforming into hair cells. We confirmed these results - obtained with *Sox9-CreER* mice - using a second Cre line, the *Lfng-CreER* line that causes efficient recombination in all supporting cell types in the organ of Corti (Basch, et al., 2016b). Under all three reprogramming conditions at both stages (P1-P8 and P8-P15), we consistently failed to see conversion of Deiters' cells or pillar cells into Myosin VIIA+ hair cells (Figure 7 – Supplementary Figure 1).

Signals from hair cells, particularly the Notch signaling pathway, are known to promote and stabilize supporting cell fate during development (Basch, et al., 2016b; Woods, et al., 2004) and induce supporting cell fate in the presence of ectopic hair cells (Kelly, et al., 2012; Woods, et al., 2004). Two types of supporting cells lie adjacent to inner hair cells: inner phalangeal and inner border cells. Both supporting cell types express the GLAST glutamate-aspartate-transporter, which plays a role in the uptake of neurotransmitters by inner hair cell ribbon synapses (Glowatzki, et al., 2006). PROX1 is a marker unique to pillar and Deiters' cells of the outer hair cell region, which is expressed until the second week of age (Bermingham-McDonogh, et al., 2006). Finally, all supporting cell types in the neonatal cochlea express the transcription factor SOX2. To determine if reprogrammed inner hair cell-like cells could promote the formation of supporting cell types normally associated with inner hair cells, we immunostained cochleae reprogrammed from P1-P8 for the supporting cell markers GLAST, PROX1, and SOX2. We found that cells in the reprogrammed GER lying beneath the reprogrammed Myosin VIIA+ hair cells expressed GLAST and SOX2 protein, but not PROX1 (Figure 7A). This suggested the reprogrammed hair cells were able to promote the formation of inner phalangeal cell and border cell-like cells from the GER, even though these cells were also expressing the reprogramming factor combinations. We observed approximately equal numbers of supporting cells in the presence of all three transcription factor combinations, suggesting that even the presence of ATOH1, GFI1, and POU4F3 in GER cells was not sufficient to prevent them from forming supporting cell-like cells when apposed to reprogrammed hair cells.

We analyzed our single-cell RNA sequencing data to identify differences in the type of GLAST+ supporting cell-like cells obtained in each condition by comparing them to wild-type (WT) inner phalangeal/border cells. Our genotype-based cell clustering data showed a significant increase in the inner phalangeal and border cell clusters between control and induced conditions (Figure 3C). A differential gene expression analysis for supporting cells in Rosa26-A vs WT, Rosa26-GA vs WT, and Rosa26-GAP vs WT indicated a common pattern of up- and downregulated genes (Figure 7B). *Cryab, Ccnd1, Rcn1,* and *Hes5* were upregulated in all three cases. *Cryab*, is a known heat shock protein with otoprotective effects during stress response and *Ccnd1*, is a cell cycle gene that is downregulated with the increasing maturity of supporting cells (Sadler, et al., 2020; Erni, et al., 2019; Laine, et al., 2010). *Hes5* is a Notch-responsive gene that is expressed in Deiters' cells and pillar cells but not inner phalangeal and border cells at birth (Tateya, et al., 2011; Doetzlhofer, et al., 2009). Its expression in the reprogrammed GLAST positive cells is likely a response to active Notch signaling induced by the ectopic hair cells to maintain supporting cell identity (Wang et al., 2010). We next examined known Notch pathway genes by performing a differential gene expression analysis between the reprogrammed GLAST+ supporting cells and reprogrammed hair cells at P8. We observed the upregulation of Notch-receiving genes (*Lfng, Notch1,* and *Hes1)* in the reprogrammed supporting cells and hair cell-specific (*Dll3, Jag2,* and *Dlk2)* Notch ligand genes in the reprogrammed hair cells (Figure 7C). This suggests that transcription factor reprogramming is capable of reconstituting the Notch signaling interactions between hair cells and supporting cells, and that these interactions are sufficient to repress the action of the three reprogramming transcription factors in the ectopically-induced supporting cells.

We repeated our supporting cell experiments by activating reprogramming at P8 and analyzing at P15. We saw evidence for the presence of ectopic GLAST+, SOX2+ supporting cell-like cells adjacent to reprogrammed hair cells in the Rosa26-GAP condition alone (Figure 8A). EdU injections given every second day from P8 to P15 showed that none of the reprogrammed hair cells or supporting cells were generated by proliferation. (Figure 8 – Supplementary Figure 1). We examined our scRNA-seq data to determine the degree to which supporting cells alter their transcriptomes in response to the three different reprogramming combinations. We performed a differential gene expression analysis of all P15 supporting cells compared to their wild-type counterparts to analyze transcriptomic changes in response to each of the three transcription factor cocktails. The most significant up and down-regulated genes are highlighted (Figure 8B), and include

Notch pathway-associated genes like *Mfng, Ccnd1, Hes5,* and *Dlk2.* In parallel to this, we also observed downregulation of many supporting cell genes such as *Ttll3, Rorb, Scd1, Scnn1b, Hhatl, Washc2* in addition to *Caecam16*. A complete description of these differentially expressed gene functions and their cell type-specific expression – extracted from the gEAR database (www.umgear.org; (Orvis, et al., 2021) is given in Figure 8 – Supplementary Tables 1 and 2.

Multi-omic analysis of the cochlea reveals hair cell loci become less epigenetically accessible in supporting cells and GER cells between postnatal days 1 and 8

The data described above suggest that both GER and supporting cells of the cochlea become more resistant to transcription factor reprogramming into hair cells during the first postnatal week. To determine if changes in the epigenetic accessibility of hair cell gene loci was partly responsible for this change, we used scMultiome to simultaneously profile gene expression and chromatin accessibility at the single cell level for each cell type of the cochlea in wild type day 1 and day 8 mice. We were able to identify most hair cell and supporting cell types of the organ of Corti as well as cells of the GER by clustering based on scRNA-seq, scATAC-seq and using “weighted-nearest neighbor” analysis (WNN; Hao, et al., 2021) which gave the clearest separation of cochlear cell types (Figure 9A). We extracted ATAC-seq profiles from 1627 distal regulatory elements associated with hair cell genes and generated heat maps to show the accessibility of these elements in GER cells and inner phalangeal cells and border cells in day 1 and day 8 cochlear tissue (Figure 9B). 498 elements showed comparable accessibility in these cell populations at both ages. However, 972 elements were significantly more accessible in the three cell populations at day 1 compared to day 8. A small number of distal elements (157) appeared to be somewhat more accessible in GER cells at day 8 compared to day 1. Examples of traces from some hair cell loci are shown in Figure 9C. *Hes6, Myo3b* and *Pou4f3* all showed reduced accessibility at day 8 in distal or intergenic regulatory elements at older ages. These results also provided a simple mechanistic explanation for why our three reprogramming mice - Rosa-A, Rosa-GA and Rosa-GAP – were all equally capable of generating reprogrammed hair cells in neonatal mice. At P1, our multi-omic analysis shows that the *Pou4f3* locus is epigenetically accessible in cells of the GER. We could identify accessible peaks with ATOH1 binding sites in this locus (Figure 9 – Supplementary Figure 1B and C), suggesting that activation of ATOH1 in the GER at this age could also induce expression of POU4F3.

Accordingly, we found that expression of ATOH1 alone induced POU4F3 protein throughout the GER with 3 days after tamoxifen addition (Figure 9 – Supplementary Figure 1A). However, in 8 day old mice, the *Pou4f3* locus was significantly less accessible in GER cells (Figure 9 – Supplementary Figure 1B), suggesting that ATOH1 alone would not be sufficient to activate these factors in GER cells. As expected, we saw no evidence for induction of POU4F3 protein when ATOH1 was activated in Rosa-A mice at P8 and POU4F3 analyzed by immunostaining at P11 (Figure 9 – Supplementary Figure 1A).

DISCUSSION

ATOH1 is the first transcription factor to be expressed in differentiating hair cells and is sufficient to generate large numbers of new hair cell-like cells when ectopically expressed in non-sensory regions of the embryonic or neonatal mouse cochlea (Kelly, et al., 2012; Liu, et al., 2012). However, its ability to reprogram these non-sensory cells to a hair cell fate declines in the first postnatal week, prompting attempts to augment its reprogramming activity with combinations of other hair cell transcription factors (Lee, et al., 2020; Menendez, et al., 2020; Yamashita, et al., 2018; Walters, et al., 2017; Costa, et al., 2015). Here, we show that the co-expression of ATOH1 with two other hair cell transcription factors, GFI1 and POU4F3, in Rosa-GAP mice can increase the efficiency of hair cell reprogramming in older animals compared to ATOH1 alone or GFI1 + ATOH1. However, the hair cells generated by reprogramming at 8 days of age- even with three hair cell transcription factors - are significantly less mature than those generated by reprogramming at postnatal day 1. By analyzing the epigenetic landscape of the cochlea over the first two postnatal weeks, we suggest that reprogramming with multiple transcription factors is better able to access the hair cell differentiation gene regulatory network, but that additional interventions may be necessary to produce mature and fully functional hair cells.

By targeting different transcription factor combinations to the same locus – *Rosa26* (Figure 1A) – we were able to directly compare the reprogramming ability of three hair cell transcription factor combinations without the confounds of variable expression levels caused by different transgene copy numbers or integration sites. Our results show that in newborn mice, activation of the reprogramming cocktails – ATOH1, ATOH1 + GFI1, and ATOH1 + GFI1 + POU4F3 - can produce equally large numbers of new inner hair cell-like cells in the greater epithelial ridge that receive neuronal input, form ribbon synapses, form immature stereocilia resembling those of endogenous hair cells at this age, and exhibit rudimentary mechanotransduction properties as shown by FM1-43 uptake (Figure 1 and 2). Moreover, these new hair cell-like cells can survive in the transformed greater epithelial ridge for at least two weeks, overriding the process of GER remodeling via apoptosis which occurs during normal cochlear development in mammals (Figure 1 – Supplementary Figure 2). Consistent with the similar morphological and functional properties of these reprogrammed cells, we found no significant differences in the transcriptomes of the reprogrammed hair cell-like cells produced by the three

transcription factor combinations when induced at P1 and analyzed a week later (Figure 3). The simplest explanation for these results is that the *Gfi1* and *Pou4f3* genes are direct transcriptional targets of ATOH1 (Yu, et al., 2021; Ikeda, et al., 2015; Hertzano, et al., 2004), and thus activation of either ATOH1 alone (or GFI1 + ATOH1) would result in the activation of all three transcription factors, together with other transcriptional effectors of the hair cell gene regulatory network. In support of this idea, we observe precocious induction of POU4F3 protein in GER cells several days after the expression of ATOH1 in Rosa-A mice. In contrast, activation of ATOH1 alone just one week later in P8 Rosa-A mice is unable to activate POU4F3 expression (Figure 9 – Supplementary Figure 1A) suggesting that components of the hair cell gene regulatory network – even those immediately downstream of *Atoh1* - become refractory to induction by ATOH1 alone in older animals.

Our data show that co-expression of GFI1 and POU4F3 with ATOH1 in the 8-day old cochlea is sufficient to generate significant numbers of reprogrammed hair cell-like cells by P15, but that ATOH1 alone or ATOH1 + GFI1 produce very few new hair cells. It is important to note that the GER is undergoing significant apoptotic remodeling at this time in response to thyroid hormone (Peeters, et al., 2015), as shown by the loss of Sox9 lineage-labeled cells from the cochlea between P8 and P15 (Figure S4A). This remodeling likely leads to a loss of cells capable of being reprogrammed by Rosa-GAP mice, which we suggest leads to an under-estimate of the reprogramming capability of Rosa-GAP mice in these experiments. Nonetheless, despite the presence of significant numbers of newly reprogrammed hair cells in ROSA26-GAP mice, our single-cell RNA-seq analysis of the new hair cell-like cells at P15 reveals no significant differences in their transcriptome compared to the small number of reprogrammed cells generated by Rosa-A and Rosa-GA mice (Figure 6C). These data suggest that although the combination of our three transcription factors can significantly increase the *efficiency* of hair cell reprogramming, they are not able to activate additional components of the hair cell gene regulatory network compared to ATOH1 alone or ATOH1 + GFI1 – in other words, the additional reprogramming factors can enhance the quantity of reprogrammed hair cells, but not their “quality”. However, this conclusion should be qualified by several considerations. First, the number of reprogrammed hair cells appearing in our scRNA-seq analysis of Rosa-A and Rosa-GA is very small, and second, since our RNA-seq analysis was performed only one week after activation of the reprogramming factors at P8, additional maturation may likely occur after longer periods. Consistent with this possibility, we note that Myosin VIIa+

cells produced by Rosa-GAP mice at P15 do not have organized actin bundles on their apical surface that can be labeled by phalloidin. Significantly, such bundles begin to appear on these GAP-reprogrammed hair cells over the following two weeks, but not in the small number of extra hair cells generated by Rosa-A mice (Figure 4 – Supplementary Figure 1B). It is also important to note that our current over-expression model causes continued expression of ATOH1 in our reprogrammed cells, whereas *Atoh1* expression is normally downregulated in hair cells shortly after they begin to differentiate. Such persistent expression may militate against full maturation of the new hair cells generated in our studies, and in previous studies that have used constitutive activation of *Atoh1* as a reprogramming strategy (Chen et al., 2021; Kelly et al., 2012; Lee et al., 2020; Liu et al., 2012; Menendez et al., 2020; Walters et al., 2017; Yamashita et al., 2018).

Supporting cells are essential for the function and survival of inner ear hair cells. During development, hair cells and supporting cells derive from a common progenitor, and the correct proportion of these two cell types is regulated by several signaling pathways, most prominently Notch signaling (reviewed by (Basch, et al., 2016a). Moreover, the generation of reprogrammed hair cells has been shown to generate new supporting cells in the surrounding tissue through non-cell-autonomous mechanisms, again including Notch signaling (Wan, et al., 2020; Zhang, et al., 2018; Stone and Cotanche, 1994). In the present study, we have shown that the production of large numbers of reprogrammed hair cell-like cells in the GER causes the induction of GLAST+ supporting cells that interleave the new hair cells. Of note, the new hair cells produced in the GER resemble inner ear hair cells, and our scRNA-seq and antibody characterization shows that the identity of ectopic supporting cells resembles border cells and inner phalangeal cells, two supporting cell types that normally surround inner hair cells. Reprogramming in the GER is, therefore, able to generate appropriately patterned and location-specific mosaics of hair cells and supporting cells similar to those that occur in vivo.

The fact that the new supporting cell-like cells retain their identity despite continuing to express hair cell reprogramming factors suggests that signaling pathways present in supporting cells can override the action of the reprogramming factors. Our data also show that some endogenous supporting cells in the organ of Corti – notably pillar cells and Deiters' cells - remain refractory to the effects of reprogramming factors at both P1 and P8. We have confirmed the refractory state of these supporting cell types with two different Cre lines, *Sox9-CreER* and *Lfng-CreER* (Figure 7 – Supplementary Figure 1). However, a recent study also expressed

ATOH1, GFI1, and POU4F3 in different populations of neonatal cochlear supporting cells and reported that some of them are capable of being reprogrammed into hair cells (Chen, et al., 2021). One of the Cre-expressing lines used to activate the reprogramming factors in the study by Chen and colleagues, *Fgfr3-iCreER*^{T2}, also expresses functional Cre recombinase in up to 30% of outer hair cells at the experimental time points and ages used in the study (Cox, et al., 2012), so it is likely that many of the labeled outer hair cells were endogenous hair cells present at the start of the experiment. Although the mice generated by Chen et al. apparently targeted the three reprogramming factors to the ROSA locus and employed a chicken beta-actin promoter in the same manner as the Rosa-GAP mice we report here, it is also possible that the two targeted lines express the reprogramming factors at different levels. Although we observe transcriptional changes in supporting cells in response to our three reprogramming combinations (Figure 8), both the hair cells and supporting cells in the organ of Corti remain healthy and viable in all conditions examined (Figure 1-8, S1-S9). In contrast, hair cell loss was observed when ATOH1, GFI1, and POU4F3 were activated by either *Fgfr3-iCreER*^{T2} or *Lgr5-CreER* mice (Chen, et al., 2021), suggesting that the levels of reprogramming factors used may be important for cochlear cell viability. Hair cell survival appears to be particularly sensitive to ATOH1 levels; hair cell loss and hearing deficits are observed in mice with only one functional ATOH1 allele, or with two hypomorphic alleles of ATOH1 (Xie et al., 2017), and so it is likely that future regenerative strategies using ATOH1 will need to calibrate the level and duration of this important transcription factor with great precision.

Several lines of evidence suggest that Notch signaling may be responsible for overriding the reprogramming ability of our transcription factor combinations. First, most organ of Corti supporting cells in neonatal mice rapidly and readily trans-differentiate into hair cells when Notch signaling is blocked (Jiang, et al., 2014; Korrapati, et al., 2013; Mizutari, et al., 2013). Second, blocking Notch signaling with gamma-secretase inhibitors can cause ectopic supporting cells in the GER created by ATOH1 reprogramming to transdifferentiate to hair cells (Kelly, et al., 2012). Third, our scRNA-seq data suggests that elements of the Notch signaling pathway are reconstituted in the ectopic supporting cells generated in our mice (Figure 7), and in endogenous supporting cells that receive reprogramming factors from P8-P15 (Figure 8). This latter result is particularly notable, as supporting cells normally transcriptionally and epigenetically down-regulate the Notch pathway in the first postnatal week and become refractory to Notch inhibition (Tao, et al., 2021; Maass, et al., 2016; Maass, et al., 2015). Together, our data suggest that transcription factor reprogramming may

reconstitute some of the transcriptional and epigenetic regulation that normally exists between developing hair cells and supporting cells, and it will be of interest in the future to understand how fully these regulatory circuits can be established by different combinations of transcription factors. In addition to the effects of Notch signaling, our multi-omic analysis of cochlear tissue at P1 and P8 shows clearly that the chromatin of hair cell loci becomes less accessible in supporting cells and GER cells during the first postnatal week (Figure 9). This decrease in accessibility affects hair cell loci in general, but significantly is also seen in key hair cell transcription factors downstream of Atoh1, including *Gfi1* and *Pou4f3* (Figure 9 – Supplementary Figure 1A). By using a single cell multi-omic analysis, we were able to demonstrate these epigenetic changes occurring in all supporting cell and GER cell populations during the first postnatal week. We suggest that this decrease in accessibility is a second element contributing to the need for multiple transcription factors to reprogram more mature cochlear tissue.

In conclusion, our work shows that while overexpression of multiple hair cell transcription factors in the cochlea clearly promotes more efficient reprogramming in older animals, significant challenges to producing viable, functional hair cells still remain. Future work will be necessary to determine whether more functional hair cells can be generated with extra hair cell transcription factors, by epigenetic modulation of hair cell loci in supporting cells, or by actively targeting the down-regulation of supporting cell genes during reprogramming. Finally, we emphasize that our present work focuses exclusively on the intact organ of Corti. We currently do not know what effect the acute and long-term pathological consequences of hair cell loss in the cochlea will have on the efficiency and fidelity of hair cell reprogramming, and addressing this question will be critical to promoting functional hair cell regeneration in the mammalian cochlea.

MATERIALS AND METHODS

Targeting of the ROSA locus:

The three conditional lines for transcription factor overexpression (Rosa-A, GA, GAP) were constructed by modifying the *Ai3* targeting construct (Addgene #22797; (Madisen, et al., 2010). The EGFP insert in *Ai3* was removed by FseI digestion and replaced with coding regions for the following: ROSA-A: *Atoh1* fused to EGFP (Rose, et al., 2009); ROSA-GA: *Gfi1* and *Atoh1-EGFP* separated by a GSG-P2A sequence; ROSA-GAP: *Gfi1*, *Atoh1-EGFP,* and *Pou4f3* separated by GSG-P2A sequences. The targeting constructs were digested with PacI and AscI to separate the construct from the homology arms and cloned into a p15a-based targeting vector containing homology arms for the ROSA26 locus (5': 1057bp; 3': 1231bp). Linearized targeting constructs (2µg) were electroporated into AB2.2 ES cells with 20µg of a pX330 plasmid (Addgene # 42230) expressing Cas9 and a sgRNA sequence to target the ROSA26 locus just inside the 5' homology arm: ACTGGAGTTGCAGATCACGA *GGG* (PAM sequence is shown in italics). 48 Neomycin-resistant clones were picked, verified for correct targeting of the ROSA26 locus, expanded, and injected into 129 blastocysts to create chimeras, which were then bred to C57Bl6 mice to establish germline founders.

Experimental animals:

All mouse experiments were performed at Baylor College of Medicine and approved by the Institutional Animal Care and Use Committee (IACUC). In addition to the *Rosa26*-targeted mice described above, we also used several lines available from the Jackson Laboratory: *Sox9-CreER*^{T2} mice (*Tg(Sox9-creERT2)1Msan/J;* stock# 018829; RRID:IMSR_JAX:018829), *Lfng-CreER* mice (Tg(Lfng-cre/ERT2)1Mmsa/J; stock# 035554; RRID:IMSR_JAX:035554), *Ai3* EGFP Cre reporter mice (Cg-*Gt(ROSA)26Sor*$^{tm3(CAG-EYFP)Hze}$/J; stock #007903; RRID:IMSR_JAX:007903) and *Ai9* tdTomato Cre reporter mice (Cg-*Gt(ROSA)26Sor*$^{tm9(CAG-tdTomato)Hze}$/J; stock# 007909; RRID:IMSR_JAX:007909). *Ai3* and *Ai9* mice are described in (Madisen, et al., 2010). For single-cell RNA sequencing work, we incorporated the *Ai9* reporter allele into our three types of crosses to yield mice of the genotypes *Sox9-CreER*^{T2}*:Rosa26*$^{Atoh1/Gfi1-Atoh1/Gfi1-Atoh1-Pou4f3}$*; Rosa26*^{tdtomato}*.* Experimental animal genotypes for all other work were *Sox9-CreER*^{T2}*; Rosa26*$^{Atoh1/Gfi1-Atoh1/Gfi1-Atoh1-Pou4f3}$

Mouse genotyping:

The following primer pairs were used for genotyping:

Sox9-CreER^{T2} mice and *Lfng-CreER* mice: Forward primer – (GCC TGC ATT ACC GGT CGA TGC AAC GA), reverse primer – (GTG GCA GAT GGC GCG GCA ACA CCA TT) yielding a band of 700bp.

Ai3 EGFP and *Ai9* tdTomato Cre reporter mice: Wild type forward primer (AAG GGA GCT GCA GTG GAG TA), wild type reverse primer – (CCG AAA ATC TGT GGG AAG TC), mutant forward primer – (ACA TGG TCC TGC TGG AGT TC), mutant reverse primer (GGC ATT AAA GCA GCG TAT CC) yielding a wild type band of 297bp and a mutant band of 212bp (https://www.jax.org/Protocol?stockNumber=007903&protocolID=28710). EGFP could also be detected with forward primer – (CGA AGG CTA CGT CCA GGA GCG CAC), reverse primer – (GCA CGG GGC CGT CGC CGA TGG GGG TGT) yielding a band of 300bp.

ROSA modified reprogramming mouse alleles: The wild type *ROSA* allele was detected using the wild type primers for *Ai3* and *Ai9* listed above, yielding a band of 297bp. The *ROSA-A* allele was specifically detected with forward primer – (AAA TGA CCA CCA TCA CCT TCG CAC C) and reverse primer – (ACG CTG AAC TTG TGG CCG TTT ACG TC), yielding a band of 483bp. The *ROSA-GA* allele was specifically detected with forward primer – (ACA TCT GCT CAT TCA CTC GGA CAC C) and reverse primer – (TTT ACC TCA GCC CAC TCT TCT GCA TG), yielding a band of 384bp. The *ROSA-GAP* allele was specifically detected with forward primer – (CTA TTT CGC CAT CCA GCC ACG TCC TTC) and reverse primer – (GAC AAC GGG CCA CAA CTC CTC ATA AAG), yielding a band of 375bp.

Tamoxifen treatment:

Tamoxifen (Sigma Aldrich) was dissolved in peanut oil at a concentration of 20mg/ml. This solution was volume optimized and injected subcutaneously at a dosage of 0.2mg/g body weight into P1 and P8 animals. Experimental and control littermates were genotyped and segregated after harvest.

Western blotting:

Cells were lysed in lysis buffer (50 mM Tris-HCl, pH 7.5, 150 mM NaCl, 0.5% Triton X-100, 5% glycerol, 1% SDS, 1x protease inhibitor cocktail). Protein concentrations were determined using a BCA assay kit (Bio-Rad).

Ten µg of protein lysate was boiled with 6X SDS sample buffer (0.5 M Tris-HCl pH 6.8, 28% glycerol, 9% SDS, 5% 2-mercaptoethanol, 0.01% bromophenol blue) and electrophoresed on a 4-15% Criterion™ Tris-HCl gel (Bio-Rad) and transferred onto a PVDF membrane. Membranes were blocked for 1 h at room temperature or overnight at 4°C using blocking buffer (5% milk in TBST). Following blocking, membranes were incubated with appropriate dilutions of primary antibody (GFP 1:500 (Santa Cruz), ATOH1 1:1000 (Proteintech), GFI1 1:1000 (Abcam), POU4F3 1:500 (Santa Cruz)) in blocking buffer for overnight 4°C on a rocker. Next, membranes were washed 3 times in TBST, 5 min each at room temperature. After this, membranes were incubated with the recommended dilution of conjugated secondary antibody in blocking buffer at room temperature for 1 hour. Membranes were washed 3 times in TBST, 5 min each. The signals were developed using Immobilon Western Chemiluminescent HRP Substrate (Millipore) and detected using ImageQuant LAS 4000 (GE Healthcare) according to the manufacturer's instructions.

Fixation, dissection, and cryosectioning:

Temporal bones from P8 and P15 mice were harvested and fixed in 4% paraformaldehyde for 2 hours at room temperature on a shaker. Fixed temporal bones were stored in 1X PBS at 4°C and microdissected with fine forceps to peel out the cochlear epithelium. In some cases, P15 temporal bones were decalcified in 0.3-0.5M EDTA (pH 8.0) for 3-4 hours at room temperature. For cryosectioning, samples were immersed in a 15% sucrose (Fisher Bioreagents #141913) solution at 4°C overnight. The temporal bones were then incubated for two hours in a sucrose-gelatin solution (7.5% gelatin (Sigma SLBX 2973) /15% sucrose and 0.0025mg of sodium azide in 1X PBS, dissolved at 65°C and stored at 37°C), followed by embedding and sectioning to give 12-14µm serial sections on a Leica CM 1850 cryostat.

Immunohistochemistry:

Whole cochlear epithelia were permeabilized with 0.5% Triton-X in 1X PBS at room temperature for 20 minutes. Sections were subject to gelatin removal by incubating in 1X PBS at 37°C for 10 minutes followed by washing. Note - The mouse Myosin VIIA and Rat SOX2 antibodies require a specific antigen retrieval step at this point. The slides/tissues were incubated in the antigen retrieval solution (10mM sodium citrate solution made by dissolving sodium citrate salt or citric acid powder in distilled water. The pH of this solution is adjusted to 6.0 using conc.HCl or NaOH respectively. 0.05% Tween 20 is added and dissolved to get a clear solution)

for 15 minutes at 80°C. The samples were cooled to room temperature without replacing the solution and washed three times. Sections were permeabilized with 0.3% Triton-X in 1X PBS at room temperature for 5 minutes. Post permeabilization, tissues (whole cochlear epithelium and sections) were washed three times with 1X PBS for 10 minutes each. Tissues were blocked with 10% goat serum for 1 hour at room temperature. Primary antibody combinations were diluted in 5% goat serum with 0.2% Triton-X and incubated overnight at 4°C. Note- For the rabbit anti-PROX1, blocking and antibody dilutions were in 10% and 1% donkey serum along with Triton X-100 respectively. For the anti-CTBP2 staining, primary antibody incubation was at 37°C overnight in a humidified chamber. After three washes with 1X PBS, tissues were incubated with fluorescently labeled secondary antibodies diluted in 5% goat serum with 0.2% Triton-X or 1X PBST and incubated for 2 hours at room temperature. Tissues were counterstained with DAPI (1:5000), washed, and dried. Tissues were mounted using the Fluormount (Southern Biotech) mounting medium, sealed with glass coverslips, and dried before imaging.

Antibodies:

Antigen	Host	Source	RRID	Dilution
Myosin VIIa	Rabbit polyclonal	Proteus Biosciences 25-6790	AB_10015251	1:300
Myosin VIIa	Mouse polyclonal	DSHB 138-1	AB_2282417	1:200
TUJ1	Mouse polyclonal	BioLegend 801213	AB_2728521	1:1000
VGLUT3	Rabbit polyclonal	Synaptic systems 135203	AB_887886	1:300
PRESTIN	Rabbit polyclonal	Gift from Dr.Jing Zheng	AB_2315199	1:1000
EpCAM/CD326	Rat polyclonal	eBioscience 17-5791-80	AB_2734965	1:300
POU4F3	Rabbit polyclonal	Proteintech 21509-1-AP	AB_2878872	1:200
GLAST	Rabbit polyclonal	Abcam ab416	AB_304334	1:300
SOX2	Rat monoclonal	Biocompare 14-9811-80	AB_11219070	1:250
SOX9	Rabbit polyclonal	Millipore Sigma AB5535	AB_2239761	1:200
PROX1	Rabbit polyclonal	Millipore Sigma AB5475	AB_177485	1:300
CTBP2	Mouse IgG1	BD Biosciences 612044	AB_399431	1:300
RFP	Chicken polyclonal	Millipore Sigma AB3528	AB_91496	1:300
GFP	Chicken polyclonal	Abcam ab13970	AB_300798	1:500
AF-488 goat anti rabbit IgG (H+L) secondary		Thermo Fisher Scientific (Invitrogen) A-11008	AB_143165	1:500

AF-488 goat anti-mouse IgG (H+L) secondary	Thermo Fisher Scientific (Invitrogen) A-11001	AB_2534069	1:500
AF-594 goat anti rabbit IgG (H+L) secondary	Thermo Fisher Scientific (Invitrogen) A-11012	AB_2534079	1:800
AF-594 goat anti-mouse IgG (H+L) secondary	Thermo Fisher Scientific (Invitrogen) A-11005	AB_2534073	1:500
AF-647 goat anti-mouse IgG1 secondary	Thermo Fisher Scientific (Invitrogen) A-21240	AB_141658	1:500
AF-488 goat anti rat IgG (H+L) secondary	Thermo Fisher Scientific (Invitrogen) A-11006	AB_2534074	1:500
AF-594 goat anti chicken IgY(H+L) secondary	Thermo Fisher Scientific (Invitrogen) A-11042	AB_2534099	1:500
Phalloidin 488	Thermo Fisher Scientific (Invitrogen) A-12379	AB_2631056	1:1000

Microscopy and image processing:

Immunostained samples were viewed on an LSM 780 confocal microscope in the Baylor Optical Imaging & Vital Microscopy Core at 20X and with emulsion oil applied to a 40X objective lens. Exposure levels were maintained between slides that were part of the same experimental batch. Maximum intensity projections obtained after processing z-stacks were processed using Adobe Photoshop CS6. Processing steps include normalization of intensity levels and derivation of 200µm lengths of the tissue measured using the scale bar option on the Zen Blue 3.1 software.

Cell number quantification:

All the images that were used for cell counting were analyzed on Zen Blue 3.1. Counting was done by using the event and marker options that sum the number of objects clicked upon. Inner hair cells, outer hair cells, and GER hair cells from 3 images were counted per genotype – WT, Rosa-A, Rosa-GA, and Rosa-GAP. Bar graphs were plotted employing the Graphpad Prism 5.0 software after performing an unpaired t-test comparing the control and each induced condition, to determine significance. For all experiments, three biological replicates (i.e. parallel measurements of biologically distinct samples) were used.

Scanning electron microscopy:

Fixing solution (all reagents from Electron Microscopy Solutions) was prepared by mixing 8% glutaraldehyde (2% final concentration), 0.6M Cacodylate buffer (pH 7.2-7.4; 0.15M final concentration) and distilled water. The temporal bones from P8 and P15 experimental animals were removed, and the apex region of each sample was punctured. The temporal bones were incubated in the SEM fixing solution for 2 hours at room

temperature. Post incubation, the temporal bones were rinsed and stored in 0.6M cacodylate buffer at 4°C. Samples were micro-dissection to expose the organ of Corti and processed with the OTOTO method for scanning electron microscopy. Tissues were then dehydrated in graded ethanol solutions, critical point dried, and mounted on a stub using silver paste. Images were taken with a TESCAN Rise scanning electron microscope.

FM 1-43 dye uptake assay:

FM 1-43 dye solution was prepared by dissolving a 10µg/µl stock of FM 1-43 (Thermo Fisher, Cat no. T35356) dye in EBSS/HBSS to a final concentration of 2µg/ml in 0.5ml. One cochlea at a time was dissected from live P8 experimental mice and placed on a glass slide. The tissue was incubated in 20 µl of the dye solution for 10-12 seconds and immediately washed with 1X PBS. The orientation of the tissue was checked followed by the addition of mounting medium. The mounted tissue was sealed with a glass coverslip and imaged under the 488 (green) channel of a Zeiss fluorescence microscope. The light intensity and brightness were normalized for images captured from different samples using the endogenous hair cells as a reference.

Cell Proliferation assay and EdU staining:

An EdU injection solution of 5mg/ml concentration was prepared by dissolving EdU powder (Thermo Fisher Scientific, #A10044) in 1X PBS pH 7.4 (Thermo Fisher Scientific, #10010023). Pups were weighed and injected with this solution at a dose of 50mg/kg body weight, subcutaneously. Injections were given twice every alternate day (9 am and 5 pm). Mice at P8 and P15 were collected, fixed, and cryosectioned following the procedures described above for IHC. EdU visualization was done using the Click-iT™ EdU Cell Proliferation Kit for Imaging, Alexa Fluor™ 488 dye (Thermo Fisher Scientific, #C10337) following the manufacturer's instruction accompanying the kit. Co-immunostaining with primary antibody for Myosin VIIA was performed as described previously in this section.

Single-cell dissociation of cochlear cells and FACS purification:

Whole ears from P8 mice were harvested and transferred to a dish of ice-cold CMF PBS. The organ of Corti was dissected from controls and experimental samples into separate microcentrifuge tubes with 0.3ml ice-cold CMF PBS placed on ice. For P15 animals, whole temporal bones were cleaned and punctured at the apex,

then placed into tubes with 0.3ml ice-cold CMF PBS. In both cases, tissue was washed twice with 0.3ml ice-cold CMF PBS and incubated in 0.3ml papain solution (20U/ml, 1mM L-Cysteine and 0.5mM EDTA; Worthington Biochemical Corporation) at 37°C for 40 minutes. The papain solution was removed carefully, and the tissue was washed twice with 0.3ml ice-cold CMF PBS containing 2-5% FBS. The tissue was triturated for 3-4 minutes by placing tubes on ice with minimal frothing, then filtered (40-micron then 35-micron filter caps – Pluriselect) into a 5ml round bottom polystyrene tube to remove clumps and bone fragments before sorting. Dissociated cells were sorted on an AriaII FACS sorter at the BCM Flow Cytometry core. The presort conditions specified for the nozzle were 20psi pressure and 100µm size respectively. TdTomato positive sorted cells were collected in DMEM with 5% FBS solution for cDNA library preparation and single-cell RNA sequencing.

cDNA library preparation:

Purified cells were counted to estimate concentration and loaded onto a 10X genomics Chromium controller to prepare single-cell 3' RNA seq libraries using the Chromium single cell 3' reagent kit v3 (10x Genomics). In brief, single cells were partitioned into GEMS (Gel Beads-In-Emulsions) that contain a gel bead with primers that include a Illumina Truseq Read 1 primer, a 16 nucleotide (nt) 10x barcode, a 12 nt unique molecular identifier and a 30 nt poly(dT) sequence and all the necessary components to perform reverse transcription. Almost simultaneously, the gel bead is dissolved and the partitioned cell is lysed releasing all the cellular RNA. Incubation of these components inside the GEM results in synthesis of full-length barcoded cDNA from the mRNA. Subsequently, the GEMS are lysed and cDNA from all the single-cells are pooled. Following cleanup using Dynabeads MyOne Silane Beads (Thermo Fisher, 370020), cDNA was amplified by PCR and fragmented to optimal size before end-repair, A-tailing, and adaptor ligation to prepare the paired end illumina libraries followed by a final PCR to amplify the library.

Single-cell RNA sequencing and analysis:

Sample QC was conducted using the NanoDrop spectrophotometer and Agilent Bioanalyzer 2100 (High Sensitivity DNA Chip, p/n 5067-4626). To quantitate the adapter-ligated library and confirm successful P5 and P7 adapter incorporations, the Applied Biosystems ViiA7 Real-Time PCR System and a KAPA Illumina/Universal Library Quantification Kit (p/n KK4824) were used. All samples were pooled at equimolar

amounts and re-quantitated by qPCR and re-assessed on the Bioanalyzer. Using the concentration from the ViiA7 TM qPCR machine above, 300pM of the pooled library was loaded onto a NovaSeq S1 flowcell (Illumina p/n 20012865), using the Standard Workflow loading conditions designated by the manufacturer and amplified by exclusion amplification (ExAMP) for patterned flowcells using the Illumina NovaSeq 6000 sequencing instrument. PhiX Control v3 adapter-ligated library (Illumina p/n FC110-3001) was spiked-in at 1% by weight to ensure balanced diversity and to monitor clustering and sequencing performance. A paired-end run, using 28 cycles for Read 1, 8 cycles for Index 1 Read and 91 cycles for Read 2 was set to achieve a minimum of approximately 300M reads per sample. FastQ file generation and QC assessment were achieved using the 10X Cell Ranger software for 10X Chromium Platforms. Sequencing data has been uploaded to the GEO database (https://www.ncbi.nlm.nih.gov/geo), accession number GSE182202.

The unique molecular identifier (UMI) count matrices were generated by aligning the raw reads to the mm10 (GRCm38) genome along with the annotation gtf file (GRCm38realease-93) (from Ensembl) using the count function of the 10x genomics Cell Ranger pipeline. Alignment, filtering, barcode, and UMI counting were also performed with Cell Ranger. The R package Seurat (v3.2) was used to process the count matrices. First, the count matrices were transformed into Seurat objects, and cells expressing less than 200 genes and genes expressed in less than 5 cells were filtered and excluded from the analysis. Another round of filtration was performed based on the distribution of the nUMI, nFeature, and percentage of mitochondrial genes expressed per cell in each dataset. Cells expressing less than 750 genes and more than 5000 genes as well as cells with greater than 30% mitochondrial genes were excluded from further analysis. The number of cells analyzed per genotype at each timepoint is given in the table below.

Age	Wildtype	Rosa26-A	Rosa26-GA	Rosa26-GAP
P8	5079	8179	3097	8957
P15	4614	4015	840	3758

Each dataset was normalized using the logNormalize function, which divided the gene counts for each cell by its total counts; followed by the identification of the top 2000 variable genes using the FindVariableFeatures function.

To identify clusters that differed between the wildtype and the transcription factor-induced datasets, an integrated analysis of the cells of all the genotypes was performed. First, we identified the integration anchors for the 4 datasets and used them to integrate the datasets using the IntegrateData function. Next, the integrated dataset was scaled by multiplying the normalized values by a factor of 10000, followed by dimensionality reduction by principal component analysis (PCA). Top 40 principal components were chosen as significant based on a Jackstraw plot and used to construct a shared nearest neighbor (SNN) graph using the FindNeighbors function. Cells were then clustered at various resolutions ranging from 0.2 to 1.0 using the Leiden algorithm in the FindClusters function of Seurat. The conserved gene markers for each cluster across the different genotypes were identified with the FindConservedMarkers function and unique gene markers for a given cluster were identified using the FindMarkers or for all clusters with FindAllMarkers function. The FindClusters and FindMarkers functions were iterated at the different resolutions until clusters with biological relevance and expected cell types were observed at a resolution of 0.8.

Each cell-type-specific cluster was identified by ranking differentially expressed genes based on the p-value of expression, average log fold change of expression, and the difference in pct1 vs pct2. A search for cell type-specific expression of the top-ranked genes yielded results unique to cell types and was thus labeled. Gene ontology analysis involved the selection of all significantly expressed genes in the hair cell clusters of the P8 and P15 datasets with a cut-off p-value of less than $1.00E^{-03}$. The analysis was done on DAVID (https://david.ncifcrf.gov/tools.jsp) with this gene list as input. Resultant GO terms and associated p-values (cut off $1.00E^{-02}$) are represented in the figure. Volcano plots for all differentially expressed genes were plotted using GraphPad Prism 5.0. All cutoffs assigned are marked with dotted lines on the plots.

Multiomic (combined scRNA- and ATAC-seq) sample processing

For Single Cell Multiome ATAC + Gene Expression (10x Genomics) experiments, wildtype mice in a mixed background of CD1 and FVB/NJ, and C57BL/6 were used. Cochlear tissue was dissected from P1 and P8 mice and enzymatically dissociated with a cocktail of 400µl of 0.25% Trypsin, 50µl of 1 mg/ml Dispase, and

50µl of 1 mg/ml collagenase for 20 minutes at 37°C. After incubation, the digested tissue was titurated 100 times using a small-bore 200µl pipette and centrifuged at 500x g for 5 minutes at 4°C. After centrifugation, the sample was processed according to the 10x Genomics protocol "Nuclei Isolation from Complex Tissues for Single Cell Multiome ATAC + Gene Expression Sequencing" (CG000375, Rev B). Briefly, the supernatant was decanted, and the cell pellet was resuspended in 1ml of NP-40 Lysis Buffer and incubated for 5 min on ice. Nuclei were filtered through a 40 micron cell strainer, and centrifuged at 500x g for 5 minutes at 4°C. The supernatant was decanted, and nuclei were resuspended in 1ml of PBS + 2% BSA and incubated for 5 min at 4C. Nuclei were centrifuged at 500x g for 5 minutes at 4°C, resuspended in 100ul of 0.1x Lysis Buffer, and mixed with a pipet. Nuclei were incubated for 2 minutes on ice, followed by the addition of 1ml Wash Buffer, mixed and centrifuged at 500x g for 5 minutes at 4°C, and resuspended in the appropriate volume of Diluted Nuclei Buffer for input into the Single Cell Multiome ATAC + Gene Expression protocol (10x Genomics). For the P1 cochlea, 6,065 nuclei were loaded. For the P8 cochlea, 9,645 nuclei were loaded.

Multiomic data processing

Raw sequencing data from both RNA and ATAC libraries in fastq format were used as input into cellranger-arc count (10x Genomics, v2.0.0) for simultaneous alignment against the mouse mm10 genome. The cellranger-arc output files 'filtered_feature_bc_matrix.h5' and 'atac_fragments.tsv.gz' were used as input into Seurat v4.1.0 for standard quality control pre-processing, resulting in 4,882 nuclei post-filtering for the P1 dataset, and 7,049 nuclei post-filtering for the P8 dataset. ATAC peaks were called using macs2 v2.1.2. Multiome datasets were clustered based on RNA, ATAC, and weighted-nearest neighbor (Hao et al, 2021) to generate UMAPs. This resulted in 20 clusters for the P1 dataset, and 19 clusters for the P8 dataset. Clusters were assigned cell types based on known cell markers. Cell barcodes from clusters of interest (P1 GER, P8 GER, P1 IPh/BC, P8 IPh, and P8 BC) were used to extract ATAC reads belonging to each respective cell type and generate a pseudobulk ATAC dataset. Peaks were called on the pseudobulk ATAC datasets and common peaks were used as input into DESeq2 v1.34.0 to scale the signal between P1 and P8 datasets. Representative signal tracks were visualized in IGV v2.4.14. ATAC peaks were filtered by hair cell enhancers previously identified (Tao et al., 2021), and intersected to find common, P1-specific, and P8-specific regions. Heatmaps were generated using deepTools v3.2.0 computeMatrix and plotHeatmap.

MATERIALS AVAILABILITY STATEMENT

The three ROSA-targeted mouse lines (ROSA-A, ROSA-GA and ROSA-GAP) are available from the corresponding author upon request.

ACKNOWLEDGEMENTS

We would like to acknowledge members of the Groves lab for their help, particularly Melissa McGovern for cryosectioning and dissection advice and Alyssa Crowder for technical assistance. We thank Gabriella Perez from the Jankowsky lab for help with the CTBP2 imaging. We thank Jing Zheng from Northwestern University for providing the Prestin antibody. We acknowledge Teng-Wei Huang for advice with immunostaining protocols.

FUNDING

The project was supported by the following grants: RO1 DC014832 (A.K.G.; subcontract to Y.R.), R21 OD025327 (R.S.R.), DC015829 (N.S.), and a Hearing Restoration Project Consortium award from the Hearing Health Foundation (A.K.G. and N.S.). The project was also supported by the following cores at Baylor College of Medicine: the Optical Imaging & Vital Microscopy Core with assistance from Jason Kirk; the Cytometry and Cell Sorting Core with funding from the CPRIT Core Facility Support Award (CPRIT-RP180672), and the NIH (P30 CA125123 and S10 RR024574) and assistance from Joel M. Sederstrom, Bethany Tiner and Amanda White; the Single Cell Genomics Core, with instrument grants from the NIH (S10OD018033, S10OD023469, S10OD025240) and P30EY002520) and assistance from Rui Chen and Yumei Li; the Genomic and RNA Profiling Core with assistance from Daniel Kraushaar; the Genetically Engineered Rodent Models core with assistance from Lan Liao and Isabel Lorenzo. The scanning electron microscopy (SEM) work was supported by the R. Jamison and Betty Williams Professorship. The SEM unit receives financial support from the University of Michigan College of Engineering and NSF grant #DMR-1625671, and technical support from the Michigan Center for Materials Characterization.

FIGURE LEGENDS

Figure 1: Non-sensory cells of the neonatal mouse cochlea can be efficiently reprogrammed to a hair cell fate with combinations of Atoh1, Gfi1 and Pou4f3 transcription factors

(A) Schematic representation of the strategy to target the Rosa26 locus to generate three conditional mouse lines for transcription factor overexpression. A modified Ai3 vector (Madisen et al., 2010) was used to target different transcription factor combinations to the *ROSA26* locus. ES cell targeting was enhanced using CRISPR-mediated cleavage with a sgRNA sequence targeting the *ROSA26* locus between the targeting homology arms (HA1 and 2). The transcription factor coding sequences were separated by GSG-T2A self-cleaving peptide sequences to generate multiple proteins from a single primary transcript.

(B) Mating schemes to express different transcription factor combinations in the cochlea. The *Sox9-CreER* mouse was bred to the three Rosa26 overexpression lines and reporters to generate experimental animals of the following genotypes: Rosa26-A (*Sox9-CreER*; $Rosa^{Atoh1GFP}$), Rosa26-GA (*Sox9-CreER*; $Rosa^{Gfi1\text{-}Atoh1GFP}$), Rosa26-GAP (*Sox9-CreER*; $Rosa^{Gfi1\text{-}Atoh1GFP\text{-}Pou4f3}$), Rosa26-EGFP (*Sox9-CreER*; $Rosa26^{EGFP}$), and Rosa26-tdtomato (*Sox9-CreER*; $Rosa26^{tdtomato}$). Animals received tamoxifen (25mg/kg body weight) at P1 and were sacrificed at P8.

(C) GFP reporter expression obtained from mating *Sox9-CreER* mice with $Rosa26^{EGFP}$mice. Fluorescence is seen in all GER cells in whole mounts and 16 µm sections. Images show GFP (green) and a DAPI nuclear stain (magenta). Scale bar: 50 µm.

(D) Large numbers of reprogrammed hair cells (white arrows) are seen in P8 cochleae extending from the organ of Corti to the interdental cell region in ROSA-A, ROSA-GA, and ROSA-GAP mice, revealed by immunostaining for Myosin VIIA (red) and Phalloidin (green).

(E) Quantification of hair cells in the P8 reprogrammed cochleae. The number of Myosin VIIA+ cells per 200 µm length of the cochlea was measured (IHC – Inner hair cells, OHC – Outer hair cells). Compared to controls, significant numbers of reprogrammed cells (300-320 per 200µm) were seen in Rosa26-A, Rosa26-GA and Rosa26-GAP genotypes (n=3 per genotype). An unpaired t-test was performed to compare hair cell numbers

between genotypes. The significant differences are represented. ****p < 0.00001. Data are presented as mean ± SEM.

Figure 2: Day 8 reprogrammed hair cells are inner hair cell-like, innervated, form ribbon synapses, possess stereociliary bundles, and show evidence of mechanotransduction activity

(A) Control and reprogrammed cochleae were immunostained for an inner hair cell-specific marker, VGLUT3, an outer hair cell-specific marker, PRESTIN, a GER specific marker, CD326/EpCAM, a neuronal marker TuJ1, a ribbon synapse-specific marker, and a hair cell marker, Myosin VIIA. The reprogrammed hair cell region is indicated (white line; eHC – ectopic hair cells). Arrows indicate individual ribbon synapse structures observed in the cell bodies of hair cells. Scale bar: 50 μm.

(B) Scanning electron micrographs (SEM) of the control and reprogrammed cochleae (500X; scale bar- 50 μm). OHC: Outer hair cell region, IHC: Inner hair cell region, GER: greater epithelia ridge region. Arrows indicate individual reprogrammed hair cells in the GER. SEM mages at 10,000X show the arrangement of stereocilia in control and reprogrammed hair cells. Arrows indicate variations in the length of individual stereocilia which are similar between control and reprogrammed hair cells. The presence of mechanotransduction activity in the induced hair cells was tested by uptake of FM1-43 dye after 10 seconds of exposure. Reprogrammed hair cells in the GER take up the dye to a lesser extent than endogenous hair cells (arrows), but more than controls, indicating some mechanotransduction channel activity.

Figure 3: Single-cell transcriptomic analysis of control and reprogrammed P8 GER cells confirm the presence of a large number of reprogrammed cells that possess hair cell-like gene signatures

(A) Mice carrying a *Sox9-CreER* allele, a *ROSA26*^{tdTomato} reporter allele, and a modified ROSA26 allele containing reprogramming factors received tamoxifen at day 1 and tdTomato+ cells were purified by FACS sorting one week later. A representative whole-mount image of a day 8 cochlea shows reprogrammed hair cells and the tdTomato reporter (scale bar: 50 μm). A representative FACS plot of dissociated cochlear cells is shown. tdTomato+ cells were collected and analyzed by scRNA-seq.

(B) UMAP plot for cells integrated and analyzed from all four genotypes (Control, Rosa26-A, Rosa26-GA, and Rosa26-GAP) purified in (A). Each identified cluster has been labeled and the anatomical location of each cluster is shown color-coded in panel (D).

(C) Genotype-wise UMAP plots highlighting the contribution of cells from each genotype in every identified cluster. The GER cluster (particularly LGER) in the control is prominent and the hair cell cluster is present only in the reprogrammed cochlear genotypes as the Sox9-CreER line does not label endogenous hair cells. IP/IB – Inner phalangeal/border, PC/DC – Pillar/Deiters' cells, HC – Hair cells, LGER – Lateral Greater epithelial ridge

(D) Schematic of an organ of Corti cross-section at P8. Unique cell types identified in the scRNA-seq clustering have been color-coded and correspond to the cluster colors in (B) and (C).

(E) Gene ontology analysis of the top differentially expressed genes in the reprogrammed hair cell-like cells from all three conditions (with respect to their expression in other cell clusters). A list of ~500 significantly expressed genes ($p < 1.00E^{-25}$) was analyzed and GO terms (Biological process; $-\log_{10}$(p-value) > 1) are shown.

Figure 4: *Gfi1, Atoh1, Pou4f3*, but not *Atoh1* or *Gfi1* + *Atoh1,* can reprogram 8-day old GER cells into hair cell-like cells

(A) Mating scheme for the targeting of transcription factors to the greater epithelial ridge and all supporting cells. The *Sox9-CreER* mouse is bred to the three Rosa26 overexpression lines in a similar manner to Figure 1A. Animals received tamoxifen (25mg/kg body weight) at P8 and were sacrificed at P15.

(B) GFP reporter expression in some lateral GER cells and all supporting cells detected by immunostaining in the organ of Corti of the *Sox9-CreER; Rosa26-EGFP* cochlea. Images show detection of GFP (green) and nuclear stain, DAPI (magenta). Scale bar: 50 μm.

(C) Quantification of hair cells in the P15 reprogrammed cochleae. The number of Myosin VIIA+ cells per 200 μm length of the organs of Corti from control, Rosa26-A, Rosa26-GA and Rosa26-GAP genotypes (n=3 per genotype) are represented. ROSA-GAP mice show approximately 50-60 ectopic hair cells, whereas ROSA-A and ROSA-GA show less than 5 ectopic cells per 200μm. An unpaired t-test was performed to compare hair

cell numbers between genotypes. Significant differences are represented. **p < 0.001. Data are presented as mean ± SEM.

(D) Rosa26-GAP mice can reprogram GER cells to hair cell-like cells. Immunostaining for Myosin VIIA (red) and Phalloidin (green) in the P15 cochleae (whole-mount organ of Corti - 200 μm length) of control, Rosa26-A, Rosa26-GA, and Rosa26-GAP mice. Arrows point to the GER region in the Rosa26-GAP cochlea, where many reprogrammed hair cells are observed.

Figure 5: Postnatal (P15) Rosa26-GAP reprogrammed hair cells are innervated and form ribbon synapses, but possess immature stereociliary bundles

(A) Control and reprogrammed cochleae immunostained for the inner hair cell-specific marker, VGLUT3, outer hair cell-specific marker, PRESTIN, neuronal marker TuJ1, ribbon synapse-specific marker CTBP2 and hair cell marker, Myosin VIIA. Arrows point to reprogrammed hair cells that are positive for Myosin VIIA in the Rosa26-GAP condition, innervation of the reprogrammed hair cells, and individual ribbon synapse structures observed in the cell bodies of endogenous and reprogrammed hair cells (Rosa26-GAP). Images show detection of described markers on a 16 μm section of the organ of Corti (control and reprogrammed). Scale bar: 50 μm.

(B) Scanning electron micrographs of reprogrammed hair cells from all three genotypes show similar hair cell-like structural features. Scanning electron micrographs (SEM) of the control and reprogrammed cochleae at 1000X (scale bar- 50 μm). Arrows indicate individual reprogrammed hair cells. OHC: Outer hair cell region, IHC: Inner hair cell region, GER: greater epithelia ridge region. SEM images at 50,000X show the kinocilium on individual hair cells and side link structures connecting hair cell stereocilia as indicated by arrows.

Figure 6: Single-cell transcriptomic analysis of control and reprogrammed cochlear cells at P15

(A) FACS-based enrichment of cochlear cells targeted for transcription factor overexpression. The breeding scheme with an experimental timeline is described followed by a representative whole mount image (bar: 50 μm) from the Rosa26-GAP cochlea. The scheme is similar to that shown in Figure 3, except that tamoxifen is injected to induce reprogramming at 8 days after birth, followed by analysis at day 15. All cells targeted for TF

overexpression are tdTomato positive (red), including reprogrammed hair cells (green). A representative FACS scatter plot of dissociated induced cochlear cells is shown.

(B) UMAP plot for cells integrated and analyzed by scRNA-seq from all four genotypes (control, Rosa26-A, Rosa26-GA, and Rosa26-GAP) purified in (A). Each identified cluster has been labeled.

(C) Genotype-wise UMAP plots highlighting the contribution of cells from each genotype in every identified cluster.

(D) Schematic of the organ of Corti cross-section at P15. Unique cell types have been color-coded and correspond to cluster colors in (B) and (C).

(E) Gene ontology analysis of the top differentially expressed genes in reprogrammed hair cells from each condition (with respect to their expression in other cell clusters for that genotype). A list of ~200 significantly expressed genes ($p < 1.00E^{-02}$) was analyzed and GO terms (Biological process, Cellular component, Molecular function; $-\log_{10}$(p-value) > 1) are represented.

Figure 7: GLAST+, SOX2+ supporting cells are induced adjacent to reprogrammed hair cells in the GER

(A) Control and reprogrammed cochleae immunostained for markers specific to inner phalangeal and border cells (GLAST), a general supporting cell marker (SOX2), pillar and Deiters' cells (PROX1), and the hair cell marker, Myosin VIIA. The reprogrammed hair cell region is indicated (line; eHC – ectopic hair cells). Images show 16 µm sections of the organ of Corti (control and reprogrammed). Scale bar: 50 µm.

(B) Differentially expressed genes from our P1-P8 scRNA-seq experiments in reprogrammed GLAST+ supporting cells are compared to control inner phalangeal/border cells. Volcano plots show common upregulated genes *Cryab, Ccnd1, Rcn1, Hes5,* and downregulated genes *Lum, Ecrg4, Gsn, Clu* (GER specific genes).

(C) Notch pathway genes are upregulated in the reprogrammed GLAST+ cells and hair cells in response to transcription factor induction at P8. UMAP plot of cells integrated from all genotypes is shown with the reprogrammed hair cells (red) and GLAST positive supporting cells (green). Average $\log_{10}$ fold change in the

expression of supporting cell-specific Notch genes – *Ccnd1, Hes5, Lfng, Jag1, Hes1, Notch1, Cdkn1a, Nrarp, Hey1, Gata3, Hes6, Heyl* and hair cell-specific Notch genes – *Dll3, Jag2, Dlk2* is represented.

Figure 8: Rosa26-GAP reprogramming from day 8 to day 15 induces ectopic GLAST+ supporting cells and up-regulates some hair cell genes in endogenous supporting cells

(A) Control and reprogrammed cochleae immunostained for markers specific to inner phalangeal and border cells (GLAST), a general supporting cell marker (SOX2), and a hair cell marker, Myosin VIIA. A reprogrammed GLAST positive supporting cell in Rosa26-GAP condition is indicated with arrows. Images show a 16 µm section of the organ of Corti (control and reprogrammed). Scale bar: 50 µm.

(B) Single-cell RNA seq analysis of supporting cells under reprogramming conditions (induction at day 8, analysis at day 15). Volcano plots show that several hair cell-specific genes and Notch pathway genes are upregulated by reprogramming factors, while several supporting cell genes are downregulated

Figure 9: Multiomic analysis of 1 and 8 day old mouse cochlea shows a loss of epigenetic accessibility of hair cell loci in GER and supporting cells.

(A) Clustering of P1 and P8 cochlear cells on the basis of scRNA-seq, scATAC-seq and weighted-nearest neighbor analyses. Different cochlear cell types can be resolved at both ages. IPh: Inner phalangeal cells; MGER: Medial greater epithelial ridge; LGER: Lateral greater epithelial ridge; IHC: Inner hair cells; OHC: Outer hair cells; GER: Greater Epithelial Ridge; BC: Border cells; DC1 and 2: Deiters' cells

(B) Heat map showing ATAC-seq peaks of 1627 distal regulatory elements identified in hair cell gene loci. ATAC-seq data was extracted from day 1 and day 8 GER cells, and inner phalangeal and border cells.

(C) Examples of changes in the accessibility of three hair cell loci (*Hes6, Myo3b, Pou4f3*) in GER cells and supporting cells in P1 and P8 mouse cochlea, measured by scATAC-seq. H3K4me1 data for each locus is taken from Tao et al., (2021). Reductions in accessibility can be seen in all three loci between P1 and P8.

SUPPLEMENTARY FIGURES

Figure 1, Supplementary Figure 1: Validation of transcription factor expression in ES cell lines used to generate *ROSA26*-targeted mice, and cochlear expression of the Sox8-CreER line

(A) Overexpression of the ROSA-A, ROSA-GA, and ROSA-GAP transcription factor combinations from the *Rosa26* locus was verified by culturing ES cells used to generate the three lines of mice with membrane-soluble TAT-Cre. Western blotting was performed after 48h with antibodies specific to ATOH1 (lane 1), GFP (lane 2), POU4F3 (lane 3), and GAPDH (loading control; lane 4).

(B) Validation of the *Sox9-CreER* transgenic mice by crossing them to the *Ai3* ROSA-EGFP reporter line. The left panels show immunostaining for SOX9 protein (green) and Myosin VIIA (red) in the P8 control. The right panels show EGFP reporter expression (green) in the Rosa26-EGFP cochlea at P8 following tamoxifen administration at P1. Images show 16 µm sections and 200 µm lengths of cochlear whole mounts. Scale bar: 50 µm.

Figure 1, Supplementary Figure 2: Reprogrammed hair cells at neonatal ages can survive until at least P15

Reprogrammed hair cells obtained by administering tamoxifen at P1 survive until at least P15. They are not subject to the apoptosis-mediated GER remodeling event that normally occurs between day 7 and day 15 (Peeters et al., 2015). Images show 200µm lengths of P15 control and experimental cochleae immunostained for Myosin VIIA (red) and fluorescently labeled phalloidin (green).

Figure 2, Supplementary Figure 1: Transcription factor induction at P1 does not influence cell proliferation in the reprogrammed cochlea

Control and Rosa26-A animals received tamoxifen (25mg/kg body weight) at P1, EdU (50mg/kg body weight) at regular intervals (P3, P5, P7 – twice per day). Animals were sacrificed at P8 for histological analysis. B: EdU incorporation (green) was observed only in cells of the spiral ganglion neuron and basal lamina regions, but not the organ of Corti (apex, middle, and base) in control and Rosa26-A animals. Images are from stained 16 µm sections with Myosin VIIA (red) indicating hair cells. No Edu+/ Myosin VIIA + hair cells can be seen in either control or experimental animals. Scale bar: 50 µm. C: Lower power images of the temporal bones analyzed at

P8 show that in addition to the SGN and basal lamina regions, extensive proliferation is observed in most parts of the temporal bone except for the cochlea epithelium.

Figure 3, Supplementary Figure 1: Examples of hair cell and LGER marker genes confirm cluster assignments in P8 cochlear cell clusters

UMAP plots (all four genotypes integrated) highlighting reprogrammed hair cell (RHC; red) and lateral GER cell (LGER; yellow) clusters. Violin plots show normalized log-transformed expression values for hair cell marker genes *Pou4f3, Pvalb, Lhx3,* and LGER marker genes *Pla2r1, Dgkb, Ces1d* in the two clusters of interest.

Figure 4, Supplementary Figure 1: Validation of Sox9-CreER activity in the cochlea from P8 to P15 and survival of reprogrammed hair cells from P15 to P29.

(A) Immunostaining for SOX9 (green) and Myosin VIIA (red) in the P8 control cochlea shows widespread SOX9 protein expression throughout the cochlear duct (left panel). The right panel shows Sox9-CreER; ROSA-EGFP mice that received tamoxifen at P8 and analyzed at P15. Most of the cochlear duct is labeled, apart from parts of the GER that undergo remodeling between P7 and P15. Images show 16 µm sections at 20x. Scale bar: 50 µm.

(B) Reprogrammed Rosa26-GAP hair cells obtained by administering tamoxifen at P8 show ectopic hair cells in the LGER region at P15, P23, and P29. By P29, most of the ectopic hair cells have organized actin bundles, revealed by enhanced phalloidin staining in the ectopic Myosin VIIA cells. Images show 200µm lengths of P15, P23, P29 control, and Rosa26-GAP cochleae immunostained for Myosin VIIA (red) and fluorescently labeled phalloidin (green).

Figure 6, Supplementary Figure 1: Examples of hair cell and supporting cell marker genes confirm cluster assignments in P15 cochlear cell clusters

UMAP plots (all four genotypes integrated) highlighting the hair cell (HC; red) and supporting cell (SC; green) clusters. Violin plots show normalized log-transformed expression values for hair cell marker genes *Pou4f3, Pvalb,* and SC marker genes GLAST, *Lfng* in the two clusters.

Figure 7, Supplementary Figure 1: Use of the a second Cre line, Lfng-CreER, confirms that pillar and Deiters' cells do not get reprogrammed into hair cell-like cells in response to transcription factor overexpression.

(A) Lfng-CreER mice crossed to ROSA-EGFP reporter mice show most supporting cells are labeled when induced with tamoxifen at P1 and analyzed at P8. A representative image of a 200µm cochlear length is shown with the reporter (green), hair cells (red – Myosin VIIA, upper panel; and phalloidin, lower panel), and DAPI (magenta).

(B) Control mice and Rosa26-A, Rosa26-GA, and Rosa26-GAP received tamoxifen at P1 or P8 and were analyzed 7 days later. Samples were labeled for Myosin VIIA (red) and Phalloidin (green). 200µm lengths are shown in all conditions. No ectopic hair cells are seen in the pillar or Deiters' cell regions in any condition. Scale bar: 50 µm.

Figure 8, Supplementary Figure 1: Transcription factor induction at P8 does not influence cell proliferation status in the control and reprogrammed cochlea at P15

Control, Rosa26-A, Rosa26-GA, and Rosa26-GAP animals received tamoxifen (25mg/kg body weight) at P8 and EdU (50mg/kg body weight) at regular intervals (P10, P12, P14 – twice per day). Animals were sacrificed at P15. EdU incorporation (green) was observed in a small number of mesenchymal cells of the temporal bone wall in all four genotypes/samples at this age, but no labeling is seen in the organ of Corti. Images are from 16 µm sections stained with Myosin VIIA (red) and DAPI (magenta).

Figure 9, Supplementary Figure 1: Endogenous Pou4f3 expression can be induced in 1 day old, but not 8 day old cochleae by reprogramming with Atoh1

A) Control and Rosa26-A animals were induced with tamoxifen at P1 or P8. Immunostaining for POU4F3 three days later at P4 (top panel) and P11 (bottom panel) revealed positive expression in the neonatal GER cells but not in the 11 day old samples. These cells were confirmed to be targeted for *Atoh1* overexpression by the *Sox9-CreER*, verified by staining for tdTomato expression in the control and Rosa26-A mice. Images show 16 µm sections at 20x. Scale bar: 50 µm. B) ATAC-seq data andH3K4me1 data from Figure 9C, combined with ATOH1 CUT&RUN data from E17.5 hair cells (Tao et al, 2021). ATOH1 binding peaks are accessible in GER

cells, inner phalangeal cells and border cells and Deiters' cells at P1, but significantly less accessible at P8. C) Heat map of ATOH1 binding sites in E17.5 hair cells, viewed for all 1627 distal regulatory elements identified as being differentially accessible in the P1 vs P8 multii-omic analysis in Figure 9B. Many of these hair cell enhancers are bound by ATOH1.

SOURCE DATA

Source data 1 for Figure 1 – Supplementary Figure 1A

Overexpression of the ROSA-A, ROSA-GA, and ROSA-GAP transcription factor combinations from the Rosa26 locus was verified by culturing ES cells used to generate the three lines of mice with membrane-soluble TAT-Cre. Western blotting was performed after 48h with antibodies specific to ATOH1, GFP, POU4F3 , and GAPDH as a loading control. The raw blots are shown.

Source data 2 for Figure 1 – Supplementary Figure 1A

Overexpression of the ROSA-A, ROSA-GA, and ROSA-GAP transcription factor combinations from the Rosa26 locus was verified by culturing ES cells used to generate the three lines of mice with membrane-soluble TAT-Cre. Western blotting was performed after 48h with antibodies specific to ATOH1, GFP, POU4F3 , and GAPDH as a loading control. The raw blots are shown with labels attached to indicate the relevant bands and the conditions used.

REFERENCES

Adler, H.J., and Raphael, Y. (1996). New hair cells arise from supporting cell conversion in the acoustically damaged chick inner ear. Neuroscience Letters 205, 17-20.

Baird, R.A., Burton, M.D., Fashena, D.S., and Naeger, R.A. (2000). Hair cell recovery in mitotically blocked cultures of the bullfrog saccule. Proceedings of the National Academy of Sciences 97, 11722-11729.

Basch, M.L., Brown, R.M., Jen, H.-I., and Groves, A.K. (2016a). Where hearing starts: the development of the mammalian cochlea. Journal of Anatomy 228, 233-254.

Basch, M.L., Brown, R.M., Jen, H.-I., Semerci, F., Depreux, F., Edlund, R.K., Zhang, H., Norton, C.R., Gridley, T., Cole, S.E., et al. (2016b). Fine-tuning of Notch signaling sets the boundary of the organ of Corti and establishes sensory cell fates. eLife 5, 1-23.

Bermingham, N.A. (1999). Math1: An Essential Gene for the Generation of Inner Ear Hair Cells. Science 284, 1837-1841.

Bermingham-McDonogh, O., Oesterle, E.C., Stone, J.S., Hume, C.R., Huynh, H.M., and Hayashi, T. (2006). Expression of Prox1 during mouse cochlear development. Journal of Comparative Neurology.

Bramhall, N.F., Shi, F., Arnold, K., Hochedlinger, K., and Edge, A.S.B. (2014). Lgr5-positive supporting cells generate new hair cells in the postnatal cochlea. Stem Cell Reports.

Cai, T., Seymour, M.L., Zhang, H., Pereira, F.a., and Groves, A.K. (2013). Conditional deletion of Atoh1 reveals distinct critical periods for survival and function of hair cells in the organ of Corti. The Journal of neuroscience : the official journal of the Society for Neuroscience 33, 10110-22.

Chen, Y., Gu, Y., Li, Y., Li, G.-L., Chai, R., Li, W., and Li, H. (2021). Generation of mature and functional hair cells by co-expression of Gfi1, Pou4f3, and Atoh1 in the postnatal mouse cochlea. Cell Reports 35, 109016.

Chonko, K.T., Jahan, I., Stone, J., Wright, M.C., Fujiyama, T., Hoshino, M., Fritzsch, B., and Maricich, S.M. (2013). Atoh1 directs hair cell differentiation and survival in the late embryonic mouse inner ear. Developmental Biology 381, 401-410.

Corwin, J., and Cotanche, D. (1988). Regeneration of sensory hair cells after acoustic trauma. Science 240, 1772-1774.

Corwin, J.T. (1981). Postembryonic production and aging of inner ear hair cells in sharks. Journal of Comparative Neurology.

Costa, A., Sanchez-Guardado, L., Juniat, S., Gale, J.E., Daudet, N., and Henrique, D. (2015). Generation of sensory hair cells by genetic programming with a combination of transcription factors. Development 142, 1948-1959.

Cotanche, D.A. (1999). Structural Recovery from Sound and Aminoglycoside Damage in the Avian Cochlea. Audiology and Neurotology 4, 271-285.

Cox, B.C., Chai, R., Lenoir, A., Liu, Z., Zhang, L., Nguyen, D.-H., Chalasani, K., Steigelman, K.A., Fang, J., Rubel, E.W., et al. (2014). Spontaneous hair cell regeneration in the neonatal mouse cochlea in vivo. Development 141, 1599-1599.

Cox, B.C., Liu, Z., Lagarde, M.M.M., and Zuo, J. (2012). Conditional gene expression in the mouse inner ear using cre-loxP. In JARO - Journal of the Association for Research in Otolaryngology.

Doetzlhofer, A., Basch, M.L., Ohyama, T., Gessler, M., Groves, A.K., and Segil, N. (2009). Hey2 regulation by FGF provides a Notch-independent mechanism for maintaining pillar cell fate in the organ of Corti. Dev Cell 16, 58-69.

Driver, E.C., Sillers, L., Coate, T.M., Rose, M.F., and Kelley, M.W. (2013). The Atoh1-lineage gives rise to hair cells and supporting cells within the mammalian cochlea. Developmental Biology 376, 86-98.

Erni, S.T., Fernandes, G., Buri, M., Perny, M., Rutten, R.J., Van Noort, J.M., Senn, P., Grandgirard, D., Roccio, M., and Leib, S.L. (2019). Anti-inflammatory and oto-protective effect of the small Heat Shock Protein Alpha B-Crystallin (HspB5) in experimental pneumococcal meningitis. Frontiers in Neurology.

Forge, A., Li, L., Corwin, J.T., and Nevill, G. (1993). Ultrastructural evidence for hair cell regeneration in the mammalian inner ear. Science.

Glowatzki, E., Cheng, N., Hiel, H., Yi, E., Tanaka, K., Ellis-Davies, G.C.R., Rothstein, J.D., and Bergles, D.E. (2006). The glutamate-aspartate transporter GLAST mediates glutamate uptake at inner hair cell afferent synapses in the mammalian cochlea. Journal of Neuroscience.

Golub, J.S., Tong, L., Ngyuen, T.B., Hume, C.R., Palmiter, R.D., Rubel, E.W., and Stone, J.S. (2012). Hair cell replacement in adult mouse utricles after targeted ablation of hair cells with diphtheria toxin. Journal of Neuroscience 32, 15093-15105.

Hao, Y., Hao, S., Andersen-Nissen, E., Mauck, W.M., 3rd, Zheng, S., Butler, A., Lee, M.J., Wilk, A.J., Darby, C., Zager, M., et al. (2021). Integrated analysis of multimodal single-cell data. Cell 184, 3573-3587 e29.

Hertzano, R., Montcouquiol, M., Rashi-Elkeles, S., Elkon, R., Yücel, R., Frankel, W.N., Rechavi, G., Möröy, T., Friedman, T.B., Kelley, M.W., et al. (2004). Transcription profiling of inner ears from Pou4f3ddl/ddl identifies Gfi1 as a target of the Pou4f3 deafness gene. Human Molecular Genetics 13, 2143-2153.

Ikeda, R., Pak, K., Chavez, E., and Ryan, A.F. (2015). Transcription Factors with Conserved Binding Sites Near ATOH1 on the POU4F3 Gene Enhance the Induction of Cochlear Hair Cells. Molecular Neurobiology 51, 672-684.

Iyer, A.A., and Groves, A.K. (2021). Transcription Factor Reprogramming in the Inner Ear: Turning on Cell Fate Switches to Regenerate Sensory Hair Cells. Frontiers in Cellular Neuroscience 15, 92.

Izumikawa, M., Batts, S.A., Miyazawa, T., Swiderski, D.L., and Raphael, Y. (2008). Response of the flat cochlear epithelium to forced expression of Atoh1. Hearing Research.

Izumikawa, M., Minoda, R., Kawamoto, K., Abrashkin, K.A., Swiderski, D.L., Dolan, D.F., Brough, D.E., and Raphael, Y. (2005). Auditory hair cell replacement and hearing improvement by Atoh1 gene therapy in deaf mammals. Nature Medicine 11, 271-276.

Jen, H.I., Hill, M.C., Tao, L., Sheng, K., Cao, W., Zhang, H., Yu, H.V., Llamas, J., Zong, C., Martin, J.F., et al. (2019). Transcriptomic and epigenetic regulation of hair cell regeneration in the mouse utricle and its potentiation by Atoh1. eLife.

Jiang, L., Romero-Carvajal, A., Haug, J.S., Seidel, C.W., and Piotrowski, T. (2014). Gene-expression analysis of hair cell regeneration in the zebrafish lateral line. Proceedings of the National Academy of Sciences 111, E1383-E1392.

Jørgensen, J.M., and Mathiesen, C. (1988). The avian inner ear - Continuous production of hair cells in vestibular sensory organs, but not in the auditory papilla. Naturwissenschaften.

Kawamoto, K., Izumikawa, M., Beyer, L.A., Atkin, G.M., and Raphael, Y. (2009). Spontaneous hair cell regeneration in the mouse utricle following gentamicin ototoxicity. Hearing Research.

Kelley, M.W., Talreja, D.R., and Corwin, J.T. (1995). Replacement of hair cells after laser microbeam irradiation in cultured organs of corti from embryonic and neonatal mice. Journal of Neuroscience.

Kelly, M.C., Chang, Q., Pan, a., Lin, X., and Chen, P. (2012). Atoh1 Directs the Formation of Sensory Mosaics and Induces Cell Proliferation in the Postnatal Mammalian Cochlea In Vivo. Journal of Neuroscience 32, 6699-6710.

Kolla, L., Kelly, M.C., Mann, Z.F., Anaya-Rocha, A., Ellis, K., Lemons, A., Palermo, A.T., So, K.S., Mays, J.C., Orvis, J., et al. (2020). Characterization of the development of the mouse cochlear epithelium at the single cell level. Nature Communications.

Kopp, J.L., Dubois, C.L., Schaffer, A.E., Hao, E., Shih, H.P., Seymour, P.A., Ma, J., and Sander, M. (2011). Sox9+ ductal cells are multipotent progenitors throughout development but do not produce new endocrine cells in the normal or injured adult pancreas. Development 138, 653-65.

Korrapati, S., Roux, I., Glowatzki, E., and Doetzlhofer, A. (2013). Notch Signaling Limits Supporting Cell Plasticity in the Hair Cell-Damaged Early Postnatal Murine Cochlea. PLoS ONE 8, e73276.

Laine, H., Sulg, M., Kirjavainen, A., and Pirvola, U. (2010). Cell cycle regulation in the inner ear sensory epithelia: Role of cyclin D1 and cyclin-dependent kinase inhibitors. Developmental Biology 337, 134-146.

Lanford, P.J., Presson, J.C., and Popper, A.N. (1996). Cell proliferation and hair cell addition in the ear of the goldfish, Carassius auratus. Hearing Research.

Lee, S., Song, J.-J., Beyer, L.A., Swiderski, D.L., Prieskorn, D.M., Acar, M., Jen, H.-I., Groves, A.K., and Raphael, Y. (2020). Combinatorial Atoh1 and Gfi1 induction enhances hair cell regeneration in the adult cochlea. Scientific reports 10, 21397.

Lelli, A., Asai, Y., Forge, A., Holt, J.R., and Géléoc, G.S.G. (2009). Tonotopic gradient in the developmental acquisition of sensory transduction in outer hair cells of the mouse cochlea. Journal of Neurophysiology.

Liu, Z., Dearman, J.A., Cox, B.C., Walters, B.J., Zhang, L., Ayrault, O., Zindy, F., Gan, L., Roussel, M.F., and Zuo, J. (2012). Age-Dependent In Vivo Conversion of Mouse Cochlear Pillar and Deiters' Cells to Immature Hair Cells by Atoh1 Ectopic Expression. Journal of Neuroscience 32, 6600-6610.

Maass, J.C., Gu, R., Basch, M.L., Waldhaus, J., Lopez, E.M., Xia, A., Oghalai, J.S., Heller, S., and Groves, A.K. (2015). Changes in the regulation of the Notch signaling pathway are temporally correlated with regenerative failure in the mouse cochlea. Frontiers in cellular neuroscience 9, 110.

Maass, J.C., Gu, R., Cai, T., Wan, Y.W., Cantellano, S.C., Asprer, J.S.T., Zhang, H., Jen, H.I., Edlund, R.K., Liu, Z., et al. (2016). Transcriptomic analysis of mouse cochlear supporting cell maturation reveals large-scale changes in Notch responsiveness prior to the onset of hearing. PLoS ONE.

Madisen, L., Zwingman, T.A., Sunkin, S.M., Oh, S.W., Zariwala, H.A., Gu, H., Ng, L.L., Palmiter, R.D., Hawrylycz, M.J., Jones, A.R., et al. (2010). A robust and high-throughput Cre reporting and characterization system for the whole mouse brain. Nature Neuroscience.

Masuda, M., Dulon, D., Pak, K., Mullen, L.M., Li, Y., Erkman, L., and Ryan, A.F. (2011). Regulation of POU4F3 gene expression in hair cells by 5′ DNA in mice. Neuroscience 197, 48-64.

Menendez, L., Trecek, T., Gopalakrishnan, S., Tao, L., Markowitz, A.L., Yu, H.V., Wang, X., Llamas, J., Huang, C., Lee, J., et al. (2020). Generation of inner ear hair cells by direct lineage conversion of primary somatic cells. eLife 9.

Mizutari, K., Fujioka, M., Hosoya, M., Bramhall, N., Okano, H.J., Okano, H., and Edge, A.S.B. (2013). Notch Inhibition Induces Cochlear Hair Cell Regeneration and Recovery of Hearing after Acoustic Trauma. Neuron 77, 58-69.

Niemiec, A.J., Raphael, Y., and Moody, D.B. (1994). Return of auditory function following structural regeneration after acoustic trauma: behavioral measures from quail. Hear Res 79, 1-16.

Obholzer, N., Wolfson, S., Trapani, J.G., Mo, W., Nechiporuk, A., Busch-Nentwich, E., Seiler, C., Sidi, S., Söllner, C., Duncan, R.N., et al. (2008). Vesicular glutamate transporter 3 is required for synaptic transmission in zebrafish hair cells. Journal of Neuroscience.

Ogata, Y., Slepecky, N.B., and Takahashi, M. (1999). Study of the gerbil utricular macula following treatment with gentamicin, by use of bromodeoxyuridine and calmodulin immunohistochemical labelling. Hearing Research.

Orvis, J., Gottfried, B., Kancherla, J., Adkins, R.S., Song, Y., Dror, A.A., Olley, D., Rose, K., Chrysostomou, E., Kelly, M.C., et al. (2021). gEAR: Gene Expression Analysis Resource portal for community-driven, multi-omic data exploration. In Nature Methods.

Pan, N., Jahan, I., Kersigo, J., Duncan, J.S., Kopecky, B., and Fritzsch, B. (2012). A Novel Atoh1 “Self-Terminating” Mouse Model Reveals the Necessity of Proper Atoh1 Level and Duration for Hair Cell Differentiation and Viability. PLoS ONE 7, e30358.

Peeters, R.P., Ng, L., Ma, M., and Forrest, D. (2015). The timecourse of apoptotic cell death during postnatal remodeling of the mouse cochlea and its premature onset by triiodothyronine (T3). Molecular and Cellular Endocrinology 407, 1-8.

Popper, A.N., and Hoxter, B. (1990). Growth of a fish ear II. Locations of newly proliferated sensory hair cells in the saccular epithelium of Astronotus ocellatus. Hearing Research.

Ranum, P.T., Goodwin, A.T., Yoshimura, H., Kolbe, D.L., Walls, W.D., Koh, J.Y., He, D.Z.Z., and Smith, R.J.H. (2019). Insights into the Biology of Hearing and Deafness Revealed by Single-Cell RNA Sequencing. Cell Reports.

Raphael, Y. (1993). Reorganization of the chick basilar papilla after acoustic trauma. J Comp Neurol 330, 521-32.

Roberson, D.W., Alosi, J.A., and Cotanche, D.A. (2004). Direct transdifferentiation gives rise to the earliest new hair cells in regenerating avian auditory epithelium. Journal of Neuroscience Research.

Roberson, D.W., Kreig, C.S., and Rubel, E.W. (1996). Light microscopic evidence that direct transdifferentiation gives rise to new hair cells in regenerating avian auditory epithelium. Auditory Neuroscience 2, 195-205.

Rose, M.F., Ren, J., Ahmad, K.A., Chao, H.T., Klisch, T.J., Flora, A., Greer, J.J., and Zoghbi, H.Y. (2009). Math1 is essential for the development of hindbrain neurons critical for perinatal breathing. Neuron 64, 341-54.

Rubel, E.W., Dew, L.A., Roberson, D.W., Warchol, M.E., Corwin, J.T., Forge, A., Li, L., and Nevill, G. (1995). Mammalian vestibular hair cell regeneration. In Science.

Ruel, J., Emery, S., Nouvian, R., Bersot, T., Amilhon, B., Van Rybroek, J.M., Rebillard, G., Lenoir, M., Eybalin, M., Delprat, B., et al. (2008). Impairment of SLC17A8 Encoding Vesicular Glutamate Transporter-3, VGLUT3, Underlies Nonsyndromic Deafness DFNA25 and Inner Hair Cell Dysfunction in Null Mice. American Journal of Human Genetics.

Ryals, B., and Rubel, E. (1988). Hair cell regeneration after acoustic trauma in adult Coturnix quail. Science 240, 1774-1776.

Sadler, E., Ryals, M.M., May, L.A., Martin, D., Welsh, N., Boger, E.T., Morell, R.J., Hertzano, R., and Cunningham, L.L. (2020). Cell-Specific Transcriptional Responses to Heat Shock in the Mouse Utricle Epithelium. Frontiers in Cellular Neuroscience.

Sheets, L., Trapani, J.G., Mo, W., Obholzer, N., and Nicolson, T. (2011). Ribeye is required for presynaptic CaV1.3a channel localization and afferent innervation of sensory hair cells. Development.

Shou, J., Zheng, J.L., and Gao, W.-Q. (2003). Robust generation of new hair cells in the mature mammalian inner ear by adenoviral expression of Hath1. Molecular and Cellular Neuroscience 23, 169-179.

Stone, J.S., and Cotanche, D.A. (1994). Identification of the timing of S phase and the patterns of cell proliferation during hair cell regeneration in the chick cochlea. Journal of Comparative Neurology.

Tang, W., Ehrlich, I., Wolff, S.B.E., Michalski, A.M., Wölfl, S., Hasan, M.T., Lüthi, A., and Sprengel, R. (2009). Faithful expression of multiple proteins via 2A-peptide self-processing: A versatile and reliable method for manipulating brain circuits. Journal of Neuroscience.

Tao, L., Yu, H.V., Llamas, J., Trecek, T., Wang, X., Stojanova, Z., Groves, A.K., and Segil, N. (2021). Enhancer decommissioning imposes an epigenetic barrier to sensory hair cell regeneration. Developmental Cell.

Tateya, T., Imayoshi, I., Tateya, I., Ito, J., and Kageyama, R. (2011). Cooperative functions of Hes/Hey genes in auditory hair cell and supporting cell development. Dev Biol 352, 329-40.

Wallis, D. (2003). The zinc finger transcription factor Gfi1, implicated in lymphomagenesis, is required for inner ear hair cell differentiation and survival. Development 130, 221-232.

Walters, B.J., Coak, E., Dearman, J., Bailey, G., Yamashita, T., Kuo, B., and Zuo, J. (2017). In Vivo Interplay between p27Kip1, GATA3, ATOH1, and POU4F3 Converts Non-sensory Cells to Hair Cells in Adult Mice. Cell Reports 19, 307-320.

Wan, L., Lovett, M., Warchol, M.E., and Stone, J.S. (2020). Vascular endothelial growth factor is required for regeneration of auditory hair cells in the avian inner ear. Hearing Research.

Woods, C., Montcouquiol, M., and Kelley, M.W. (2004). Math1 regulates development of the sensory epithelium in the mammalian cochlea. Nature Neuroscience 7, 1310-1318.

Xiang, M., Gan, L., Li, D., Chen, Z.-Y., Zhou, L., O'Malley, B.W., Klein, W., and Nathans, J. (1997). Essential role of POU-domain factor Brn-3c in auditory and vestibular hair cell development. Proceedings of the National Academy of Sciences 94, 9445-9450.

Xiang, M., Gao, W.Q., Hasson, T., and Shin, J.J. (1998). Requirement for Brn-3c in maturation and survival, but not in fate determination of inner ear hair cells. Development (Cambridge, England) 125, 3935-46.

Yamashita, T., Zheng, F., Finkelstein, D., Kellard, Z., Carter, R., Rosencrance, C.D., Sugino, K., Easton, J., Gawad, C., and Zuo, J. (2018). High-resolution transcriptional dissection of in vivo Atoh1-mediated hair cell conversion in mature cochleae identifies Isl1 as a co-reprogramming factor. PLOS Genetics 14, e1007552.

Yu, H.V., Tao, L., Llamas, J., Wang, X., Nguyen, J.D., Trecek, T., and Segil, N. (2021). POU4F3 pioneer activity enables ATOH1 to drive diverse mechanoreceptor differentiation through a feed-forward epigenetic mechanism. Proceedings of the National Academy of Sciences of the United States of America.

Zhang, J., Wang, Q., Abdul-Aziz, D., Mattiacio, J., Edge, A.S.B., and White, P.M. (2018). ERBB2 signaling drives supporting cell proliferation in vitro and apparent supernumerary hair cell formation in vivo in the neonatal mouse cochlea. European Journal of Neuroscience.

Zheng, J., Shen, W., He, D.Z.Z., Long, K.B., Madison, L.D., and Dallos, P. (2000). Prestin is the motor protein of cochlear outer hair cells. In Nature.

Zheng, J.L., and Gao, W.-Q. (2000). Overexpression of Math1 induces robust production of extra hair cells in postnatal rat inner ears. Nature Neuroscience 3, 580-586.

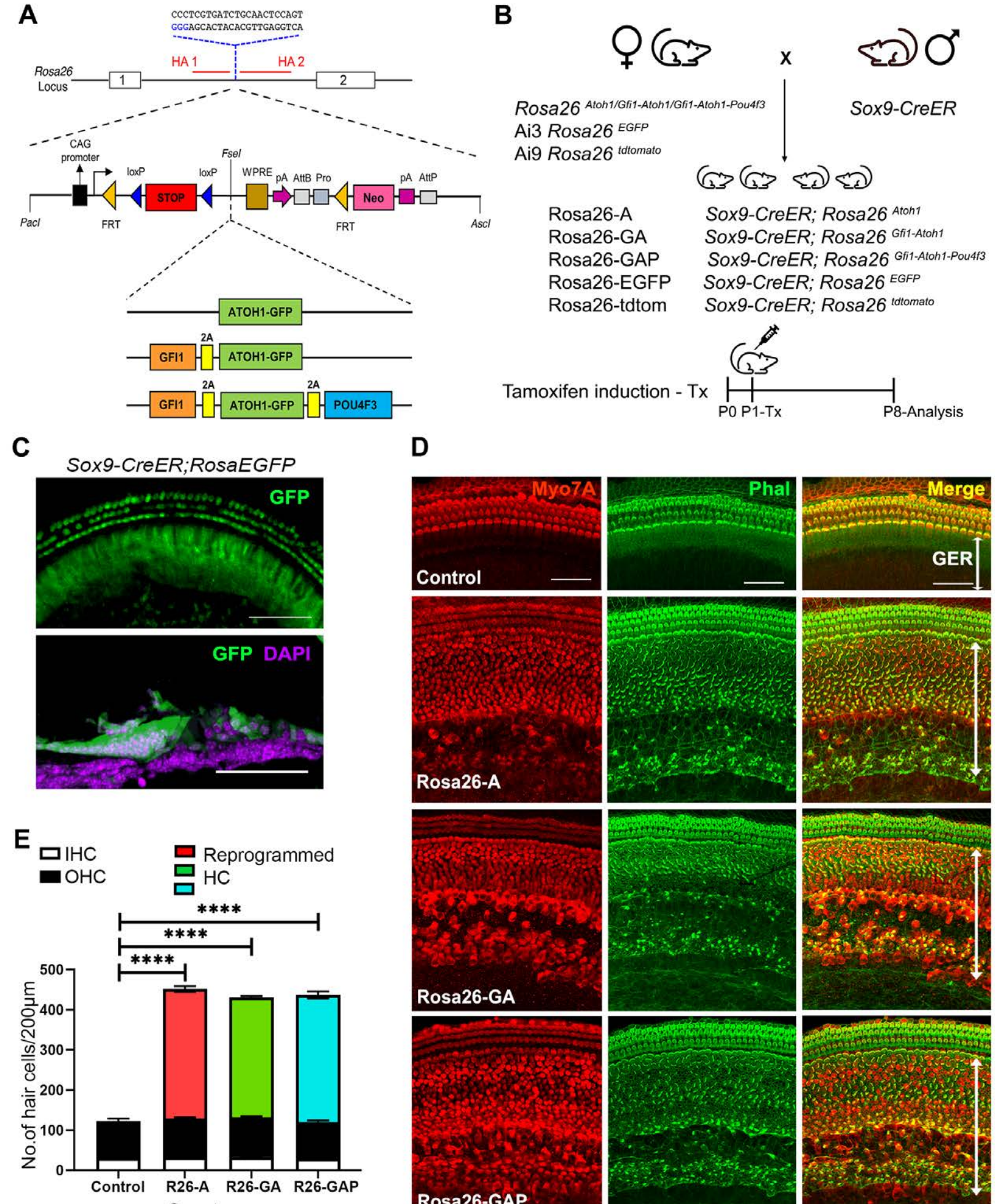

A. Validation of transcription factor overexpresion through western blot

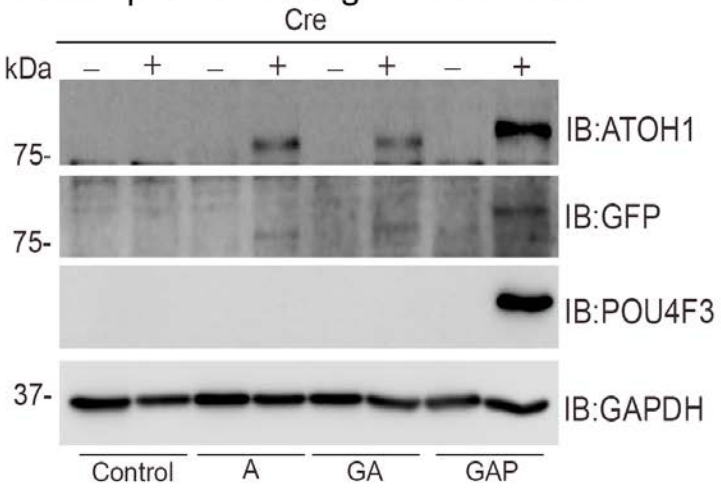

B. Comparison between *Sox9* positive cells and those targeted by *Sox9-CreER* at P8

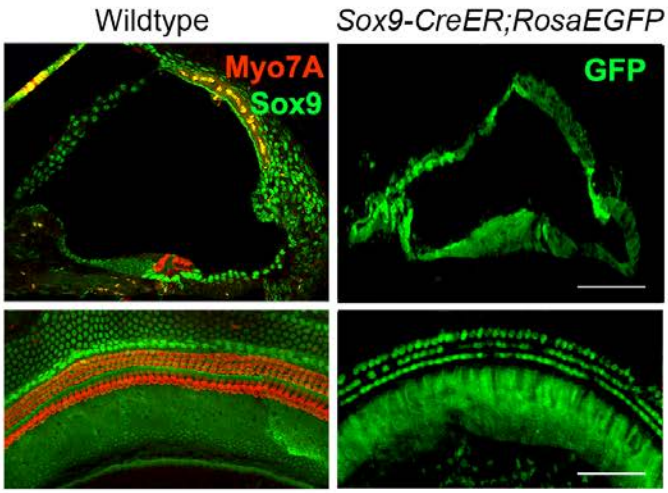

Iyer et al. Figure 1 - S1

A. Reprogrammed hair cells in the GER override apoptosis remodeling signals and survive

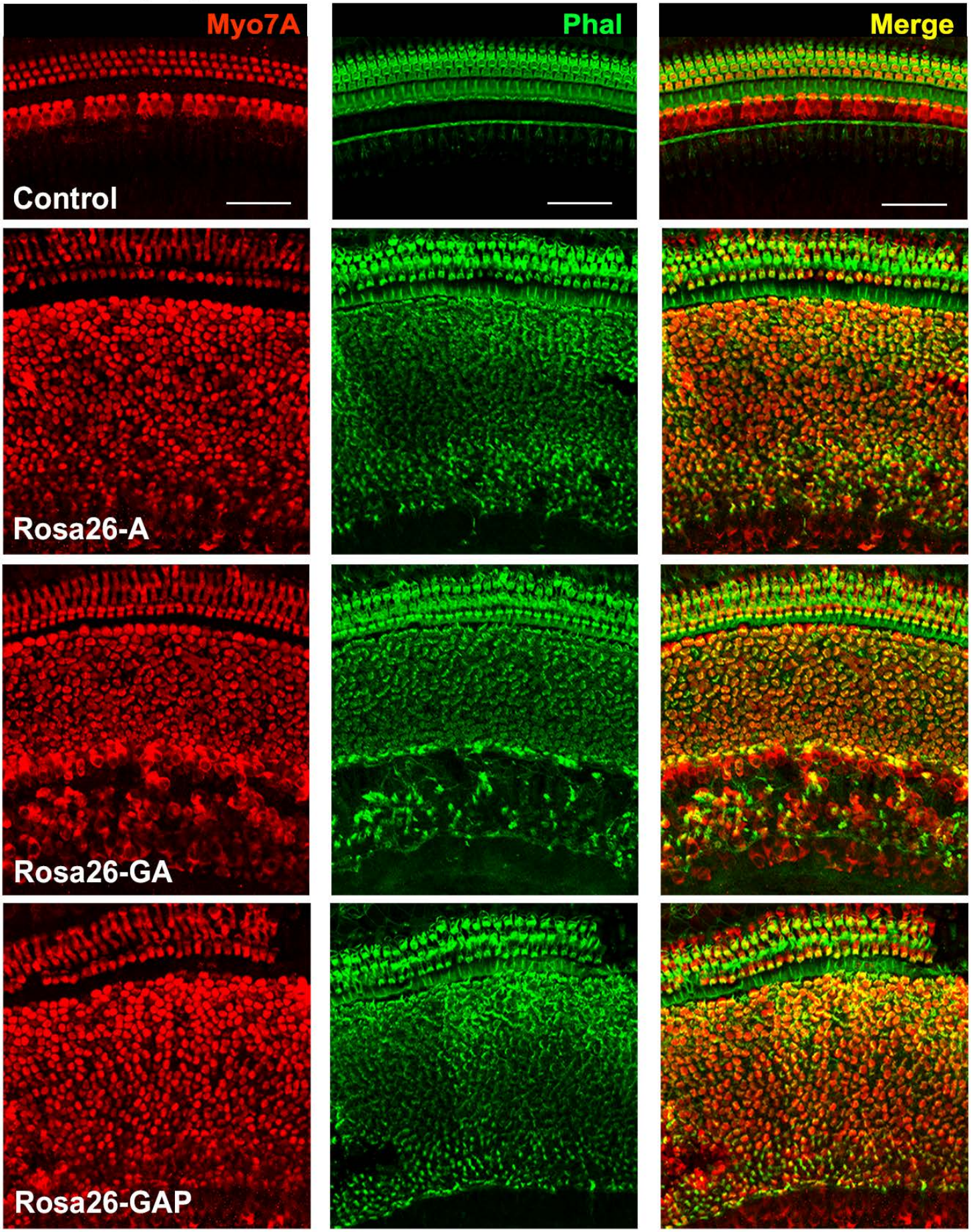

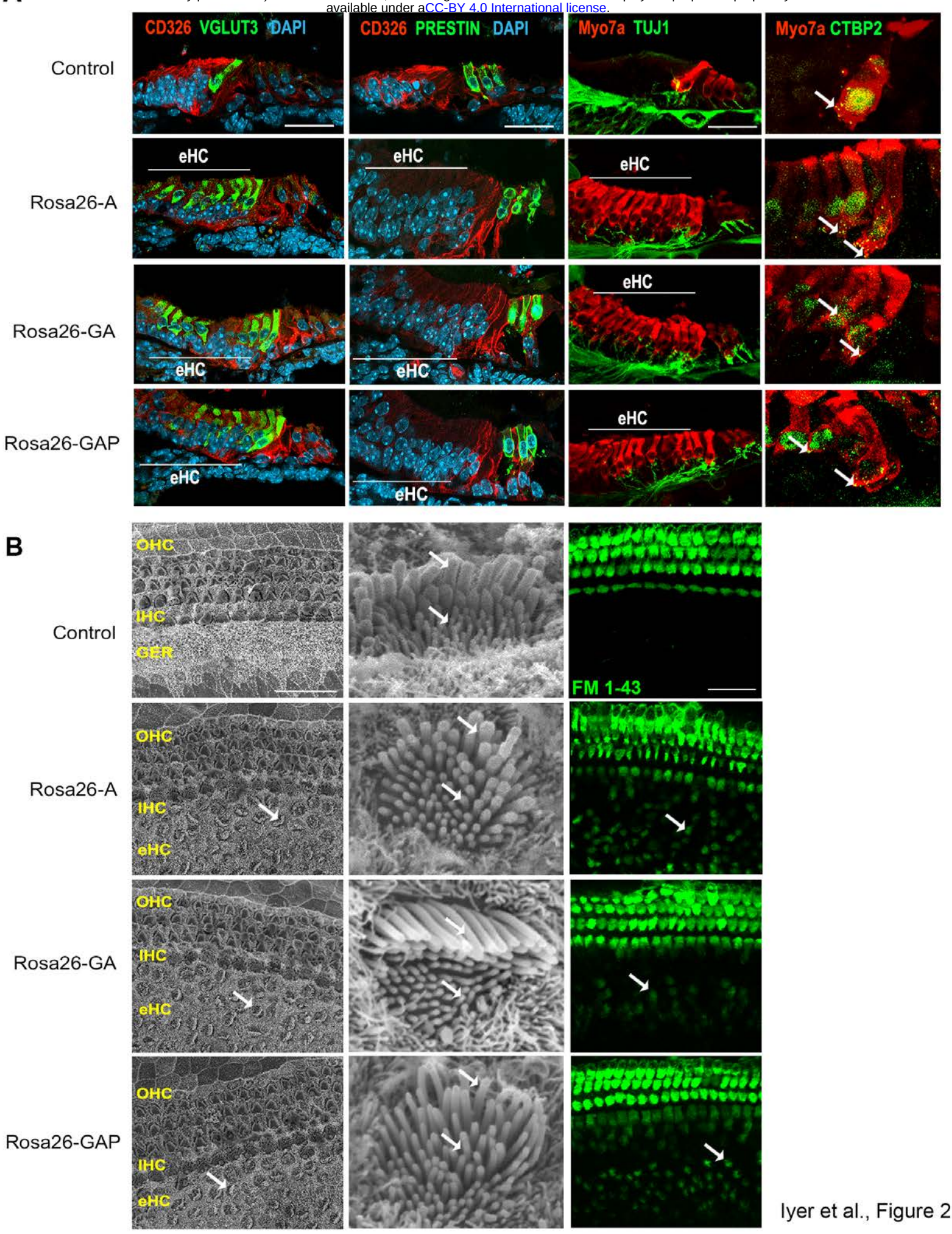

Iyer et al., Figure 2

A. EdU incorporation in the neonatal mouse cochlea on induction with Atoh1

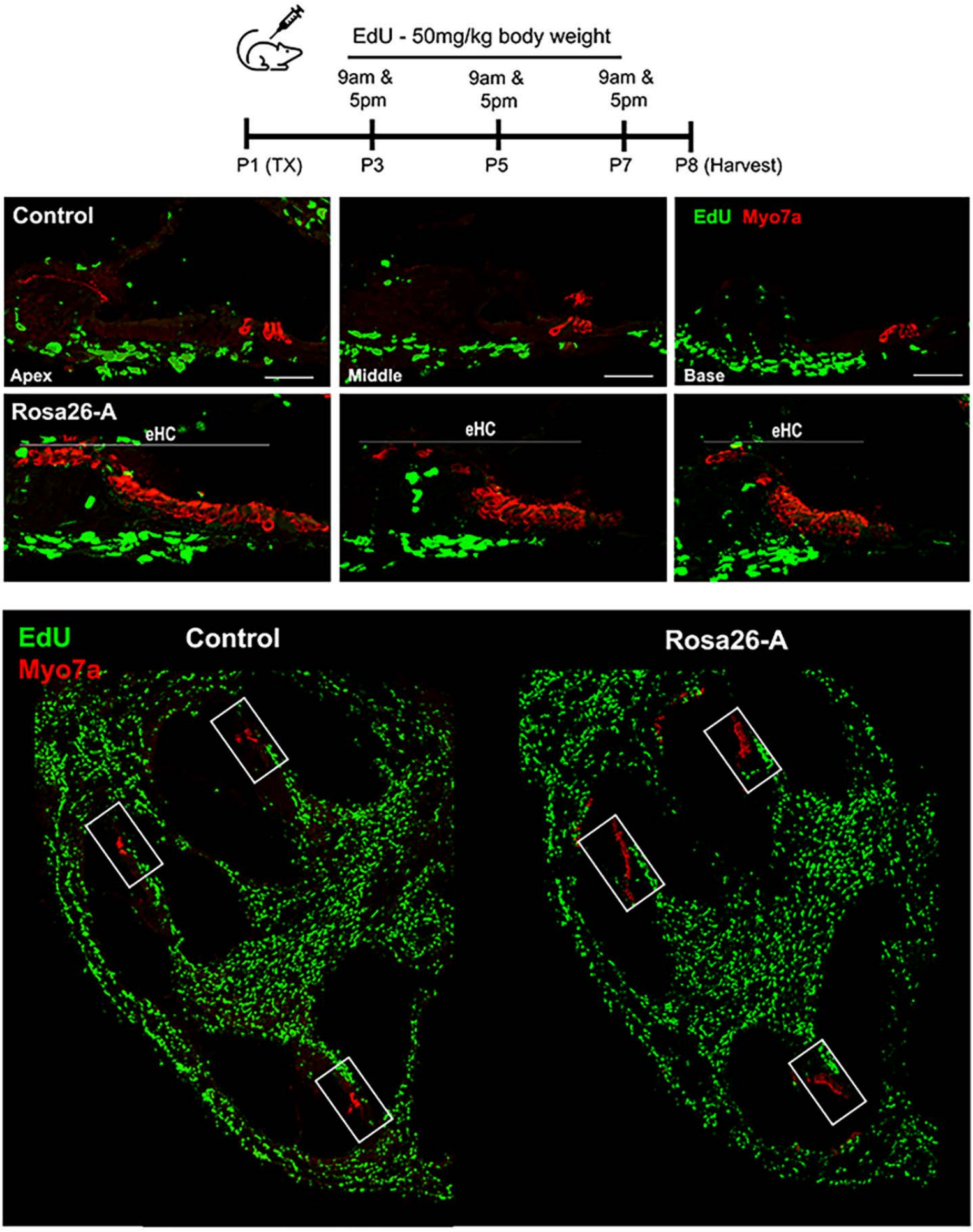

Iyer et al. Figure 2 - S1

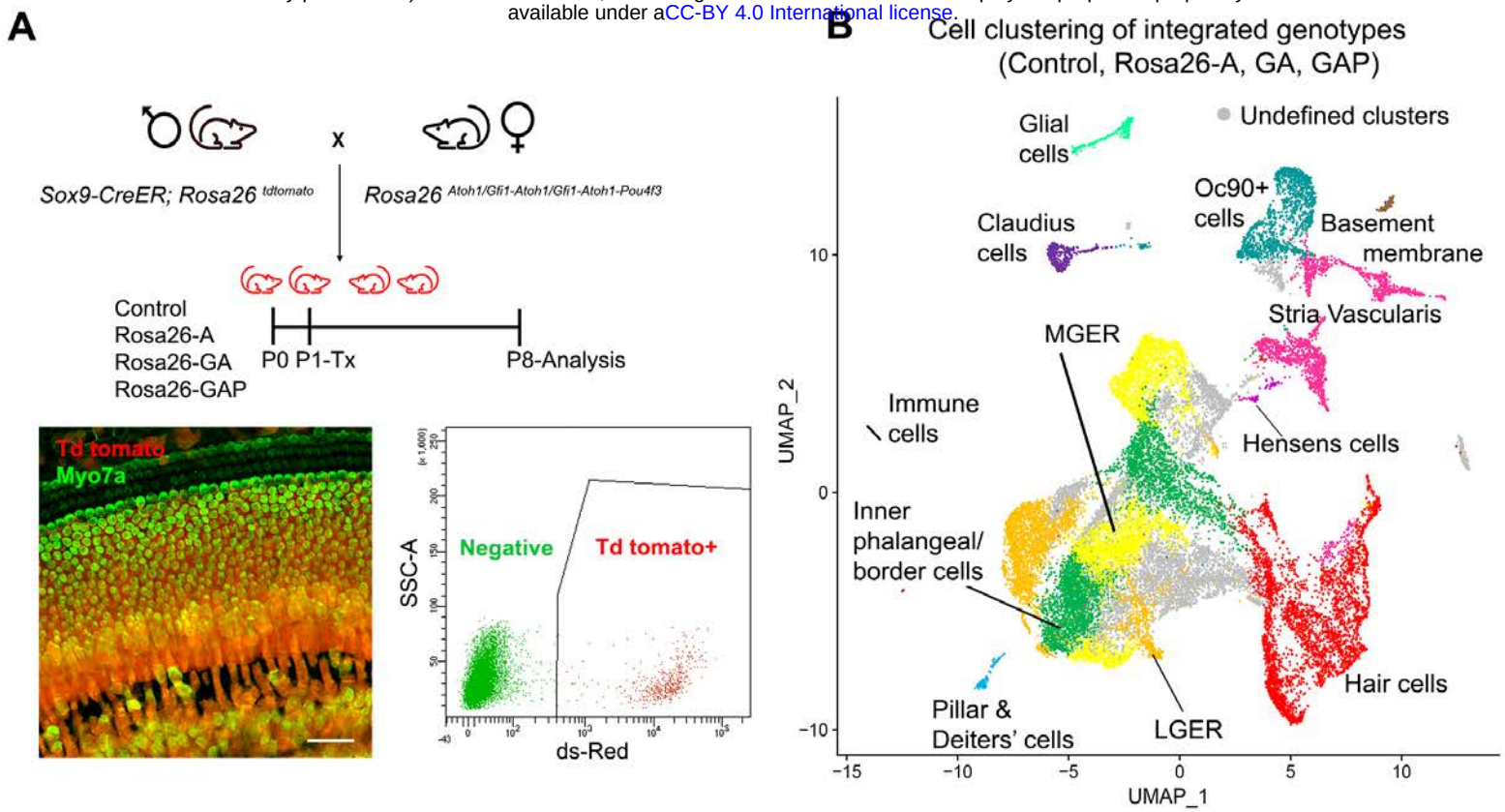

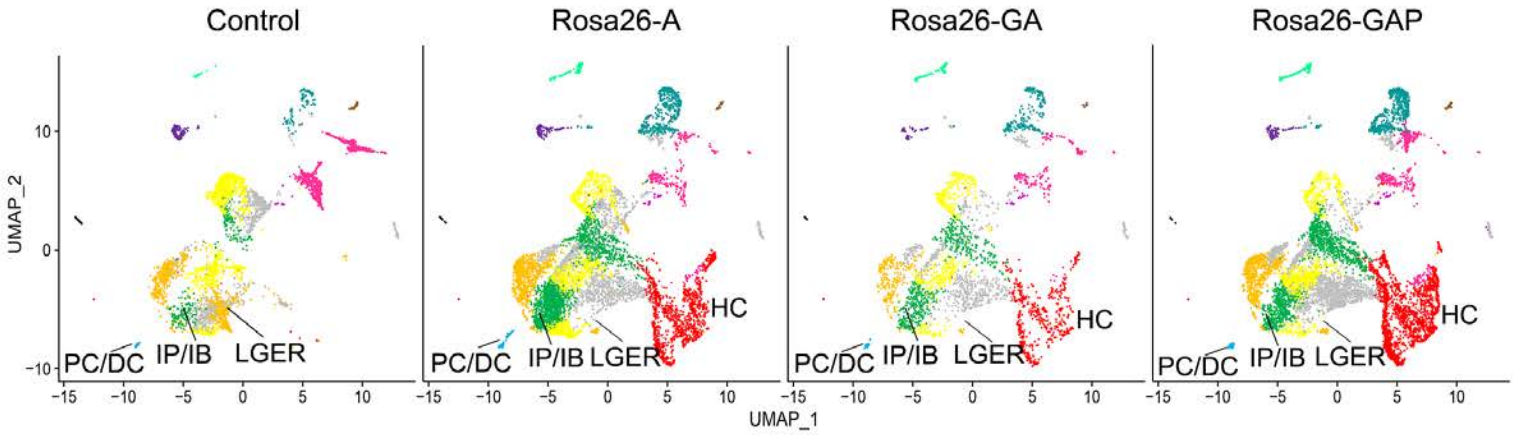

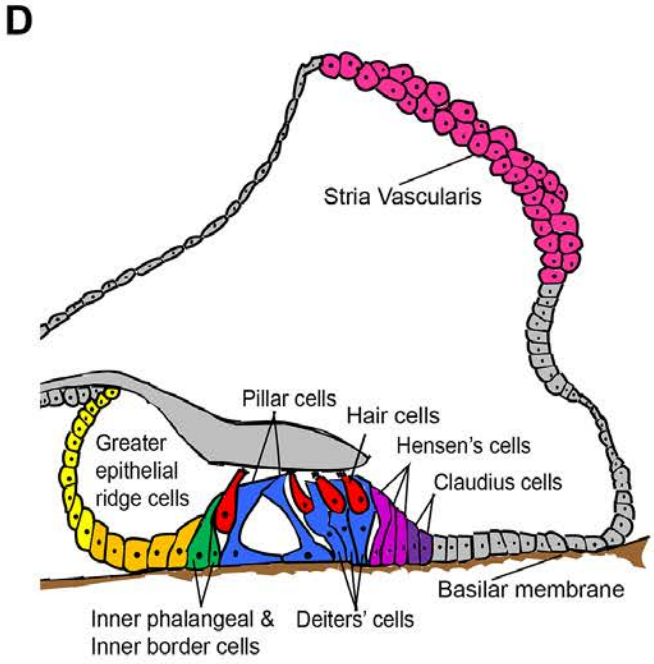

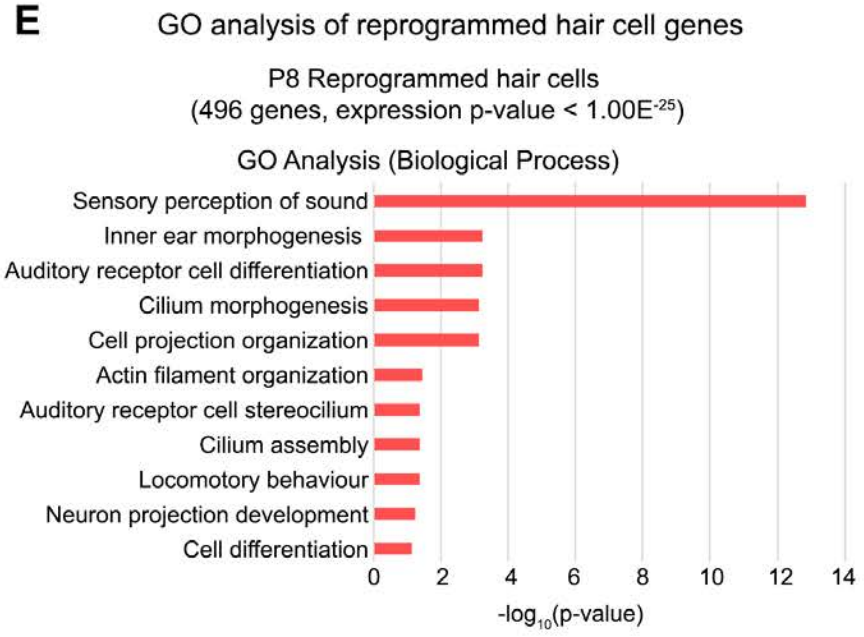

A. Cluster identification with expression of unique and common cell type specific markers

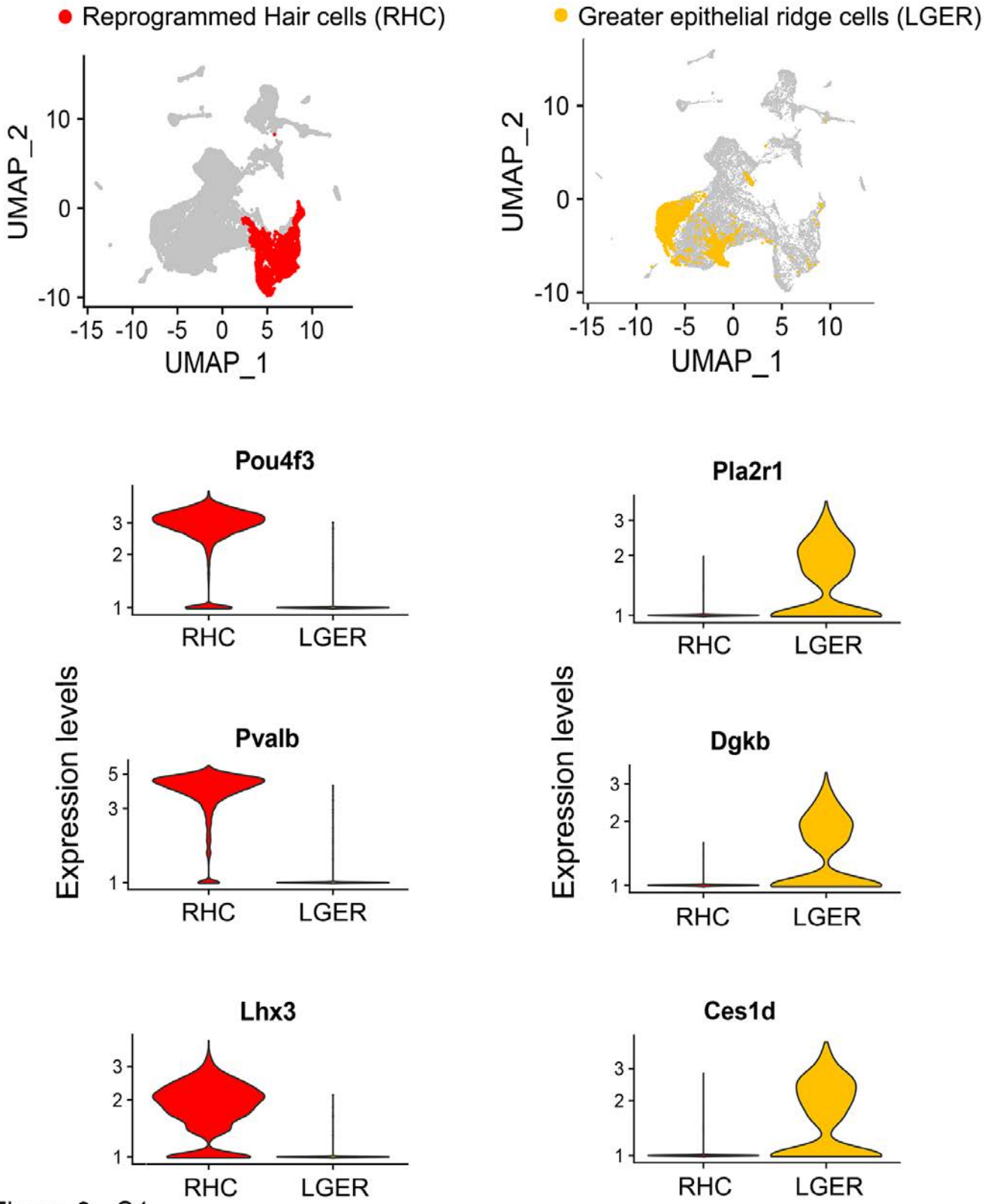

Iyer et al. Figure 3 - S1

Iyer et al. Figure 4

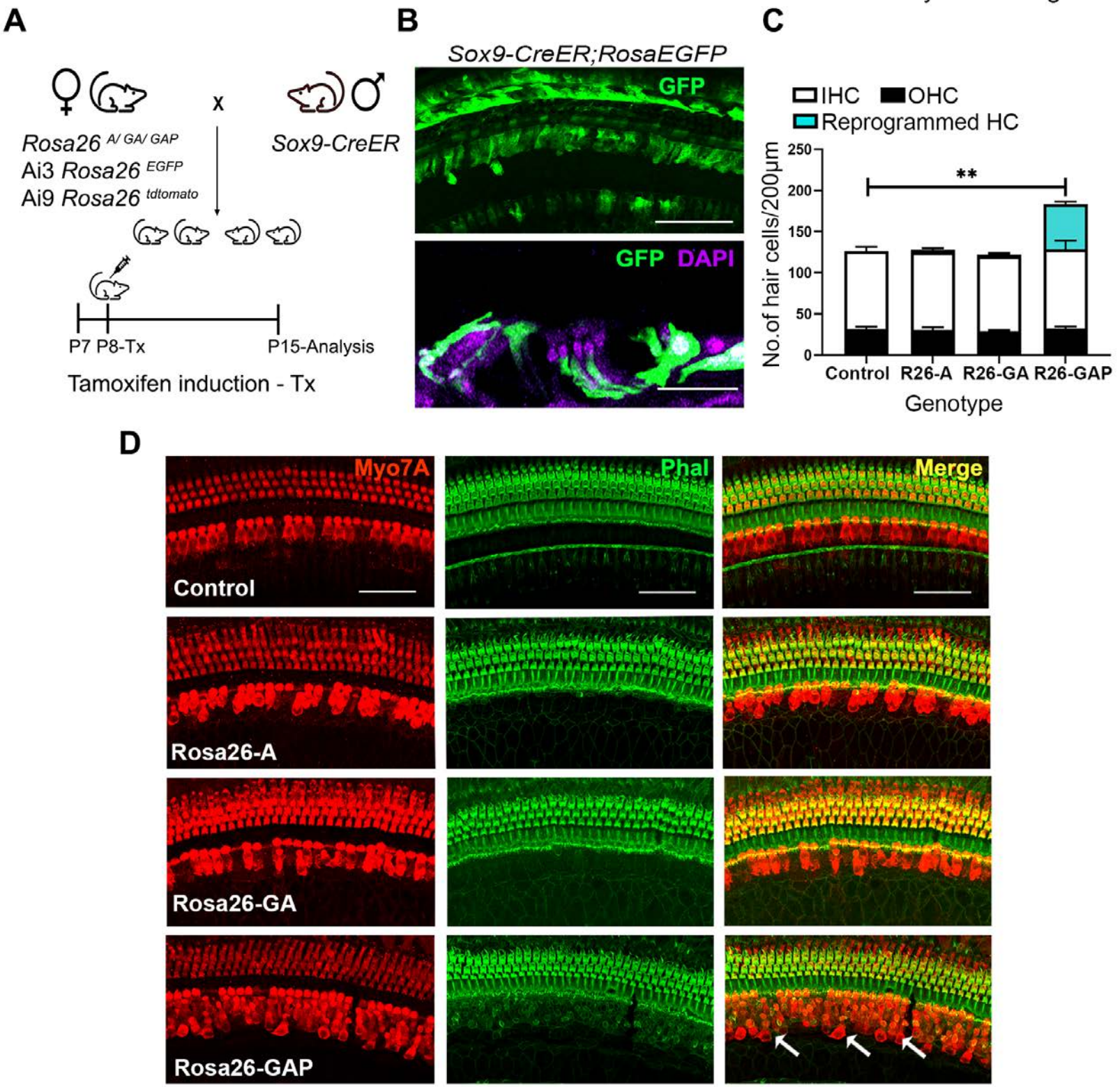

A. Comparison of P15 cochlear cells expressing *Sox9* and targeted by *Sox9-CreER*

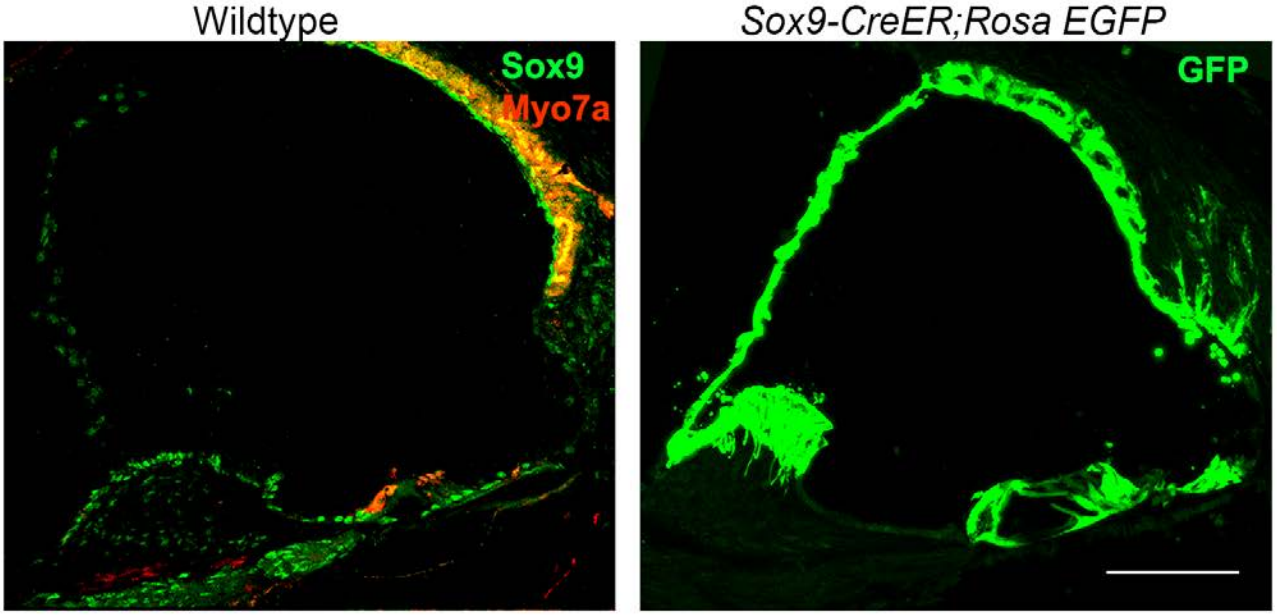

B. P15 reprogrammed hair cells in the GER mature and survive over time

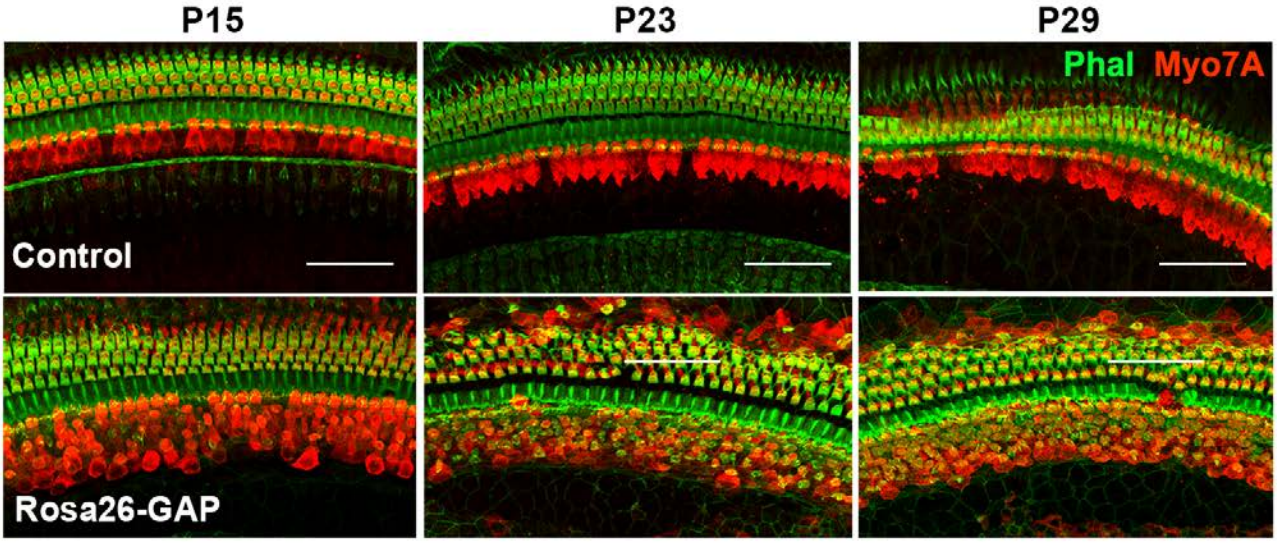

Iyer et al. Figure 4 - S1

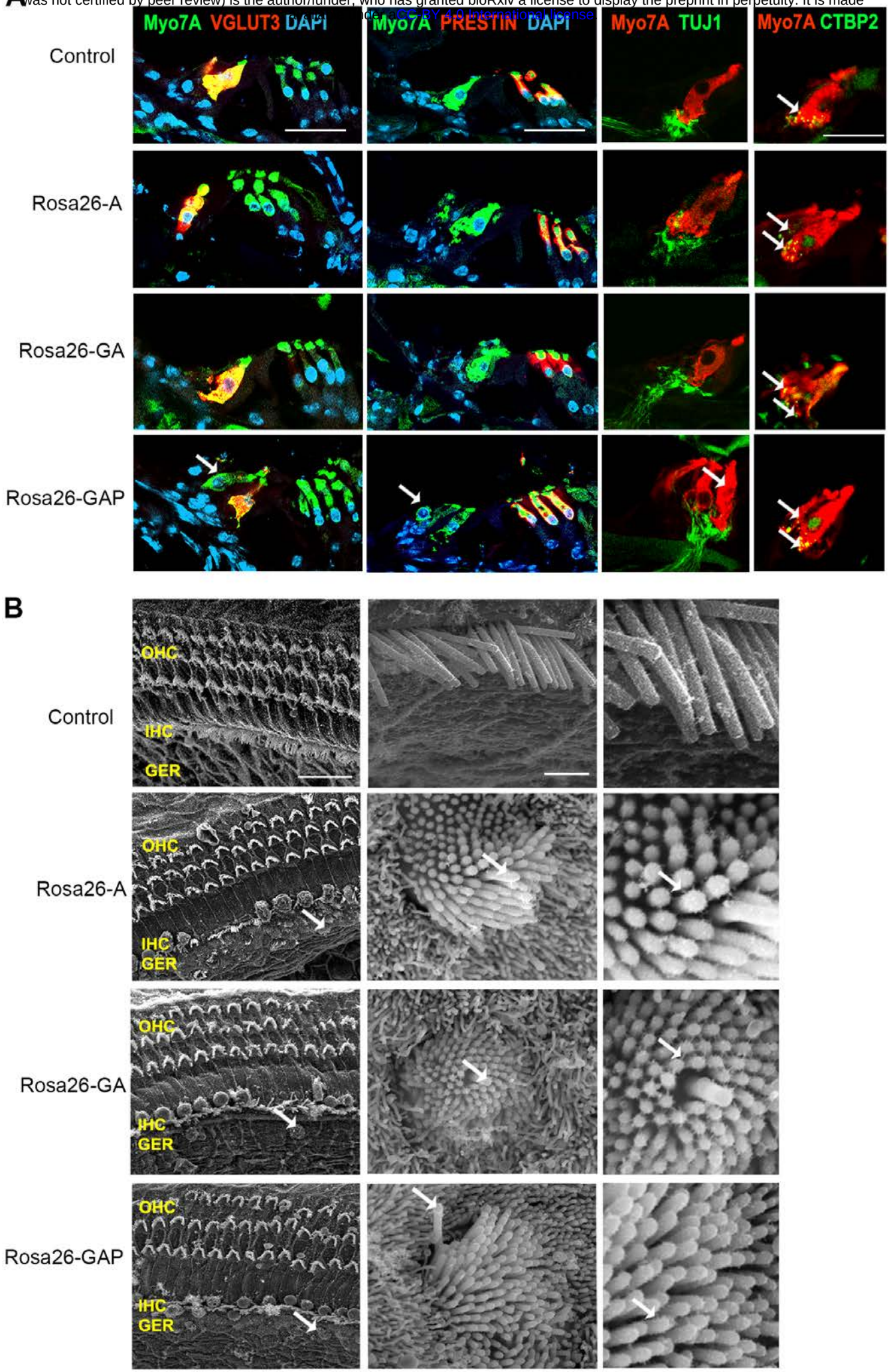

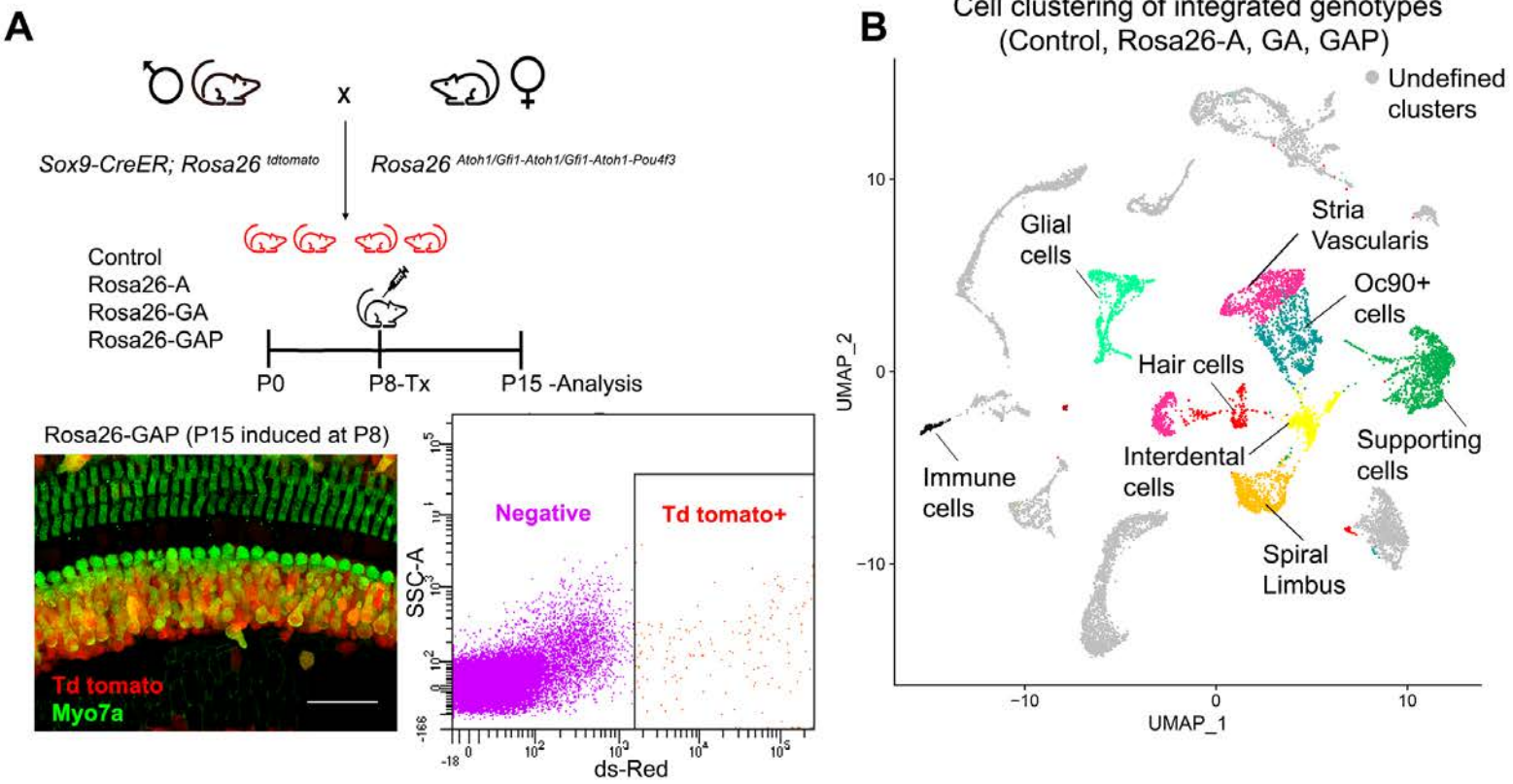

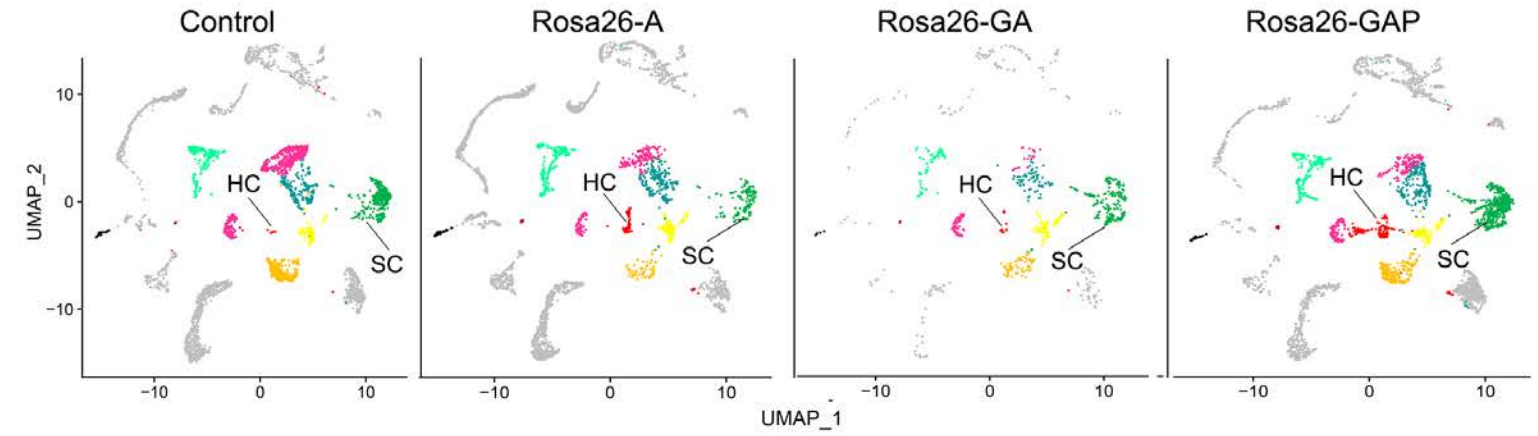

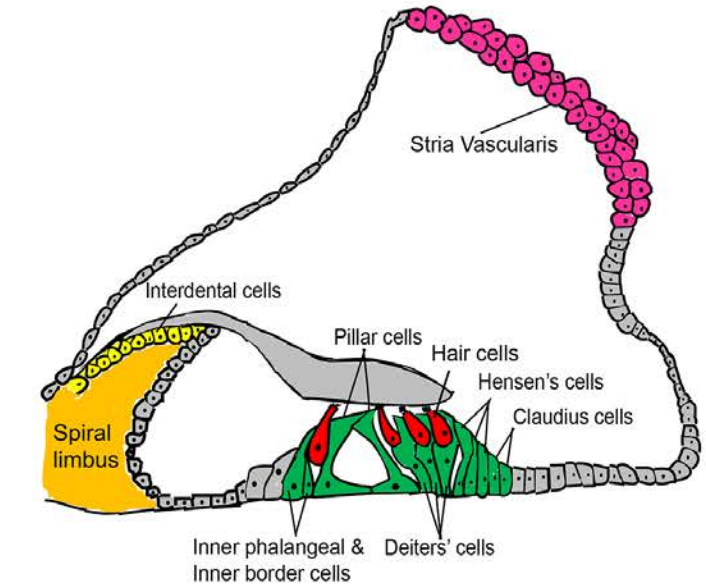

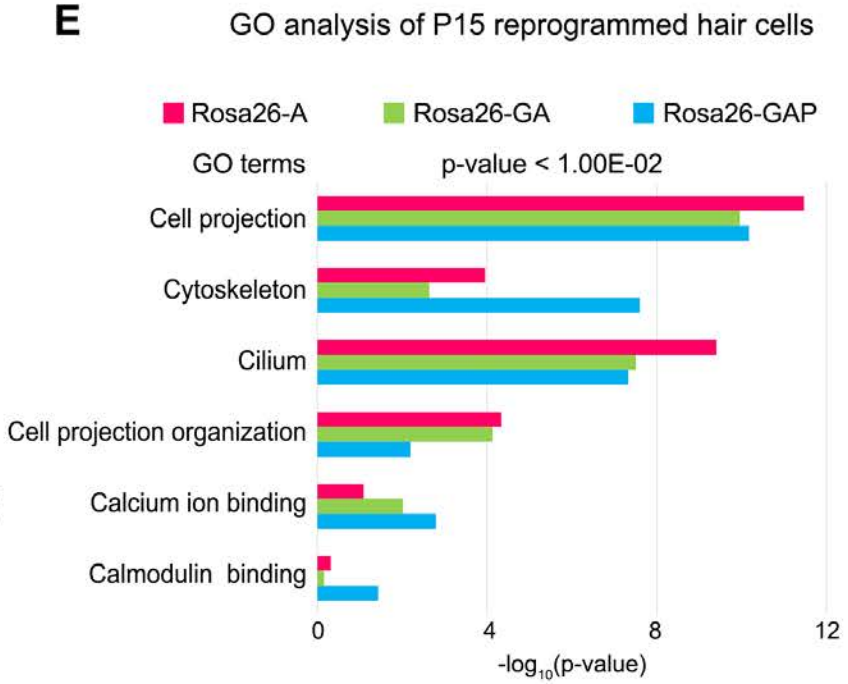

A. Cluster identification with expression of cell type specific markers

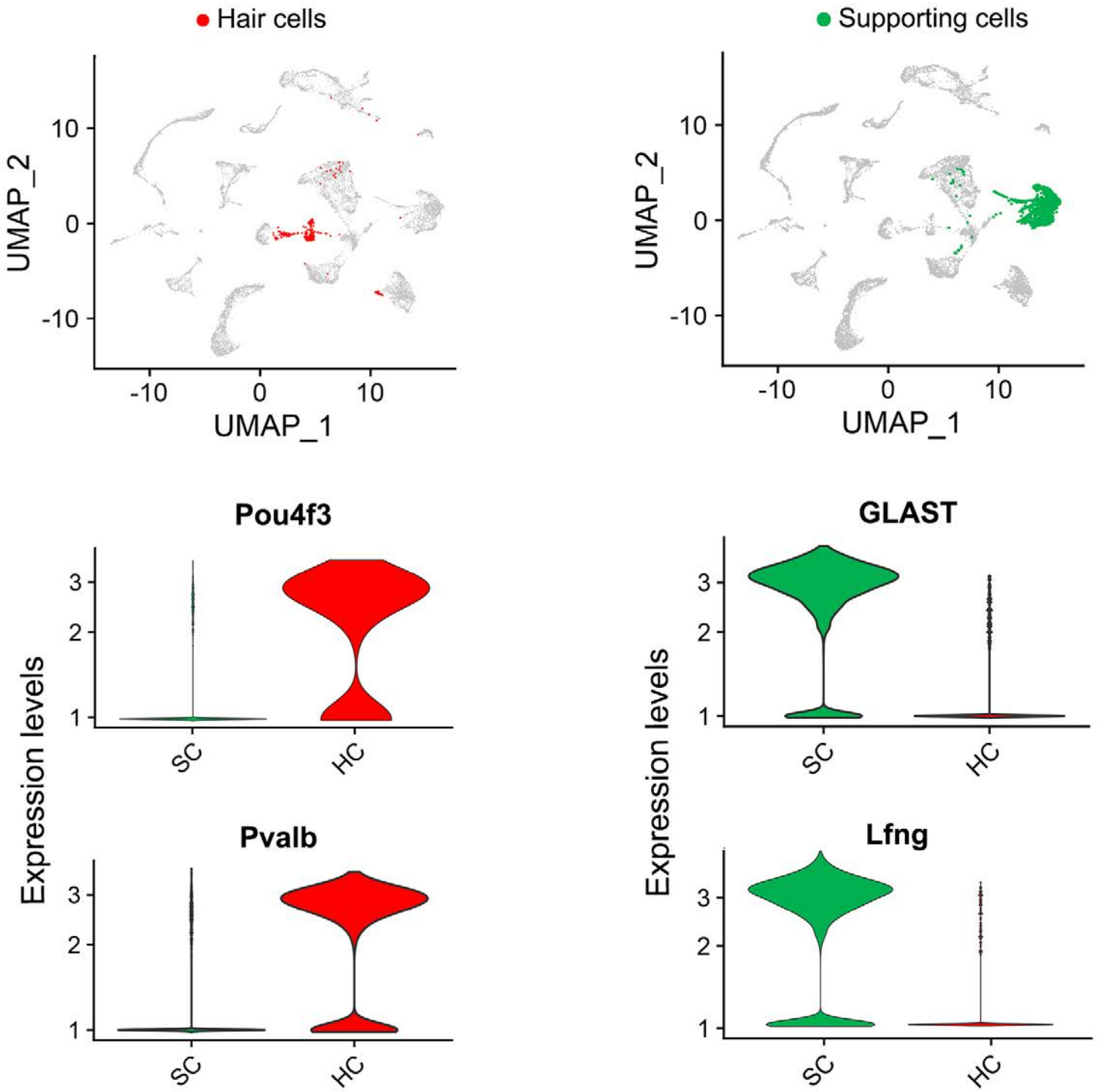

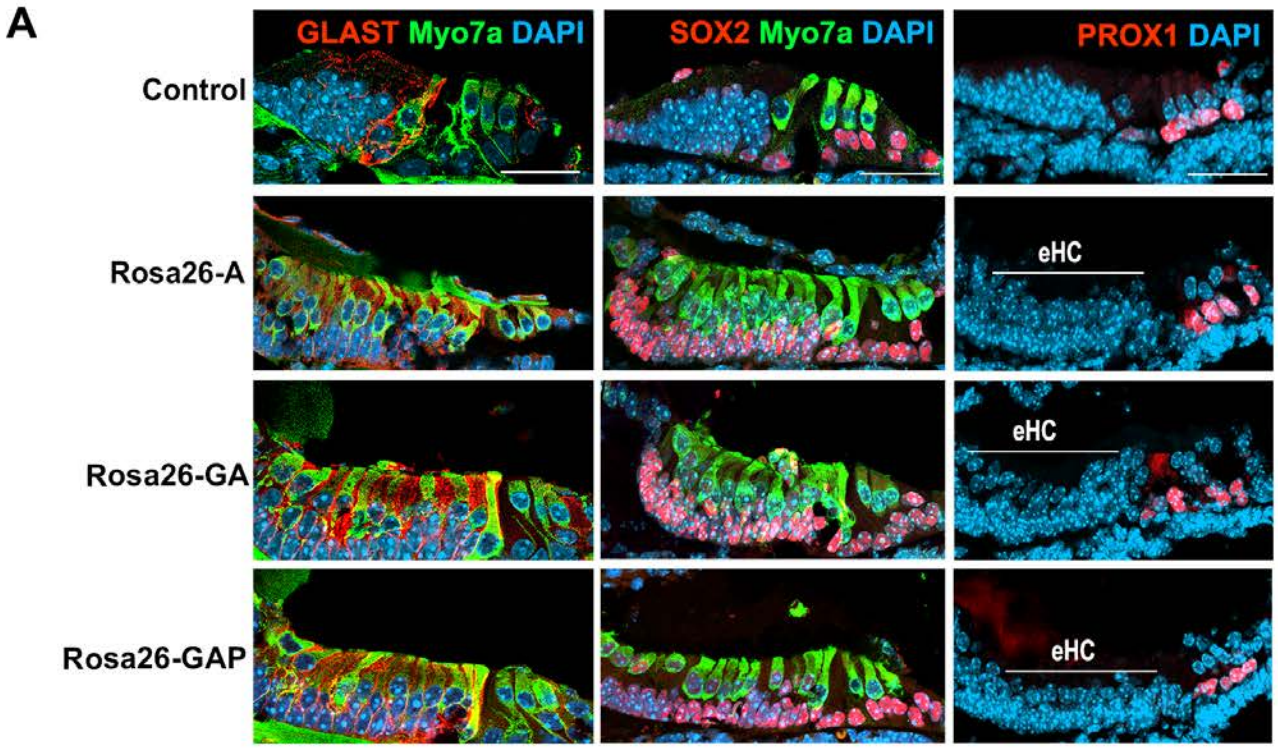

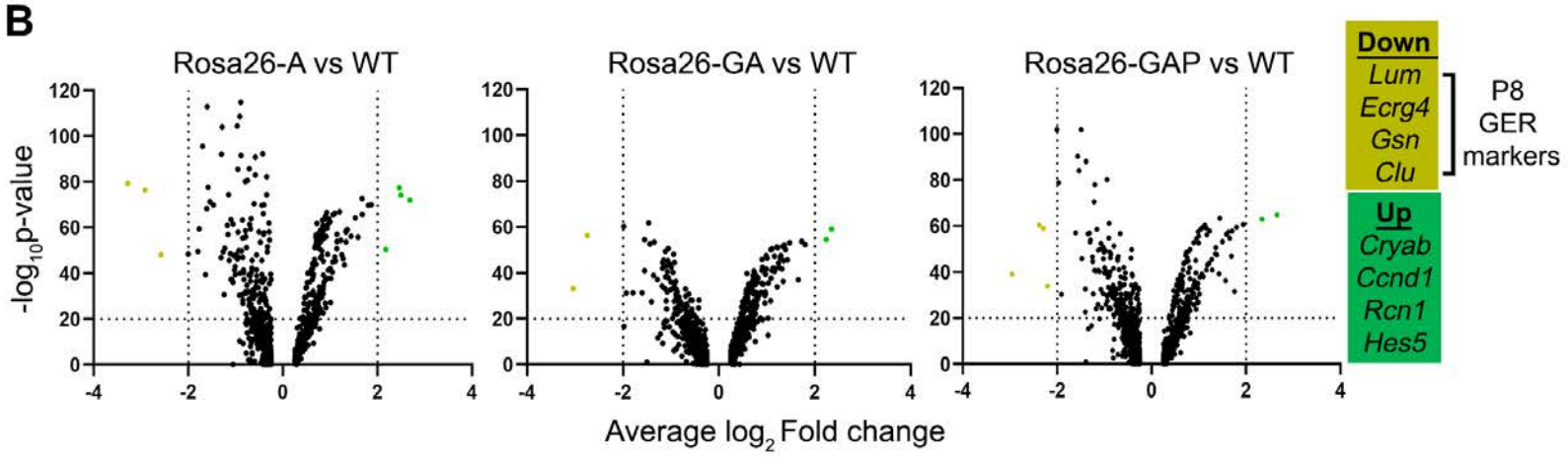

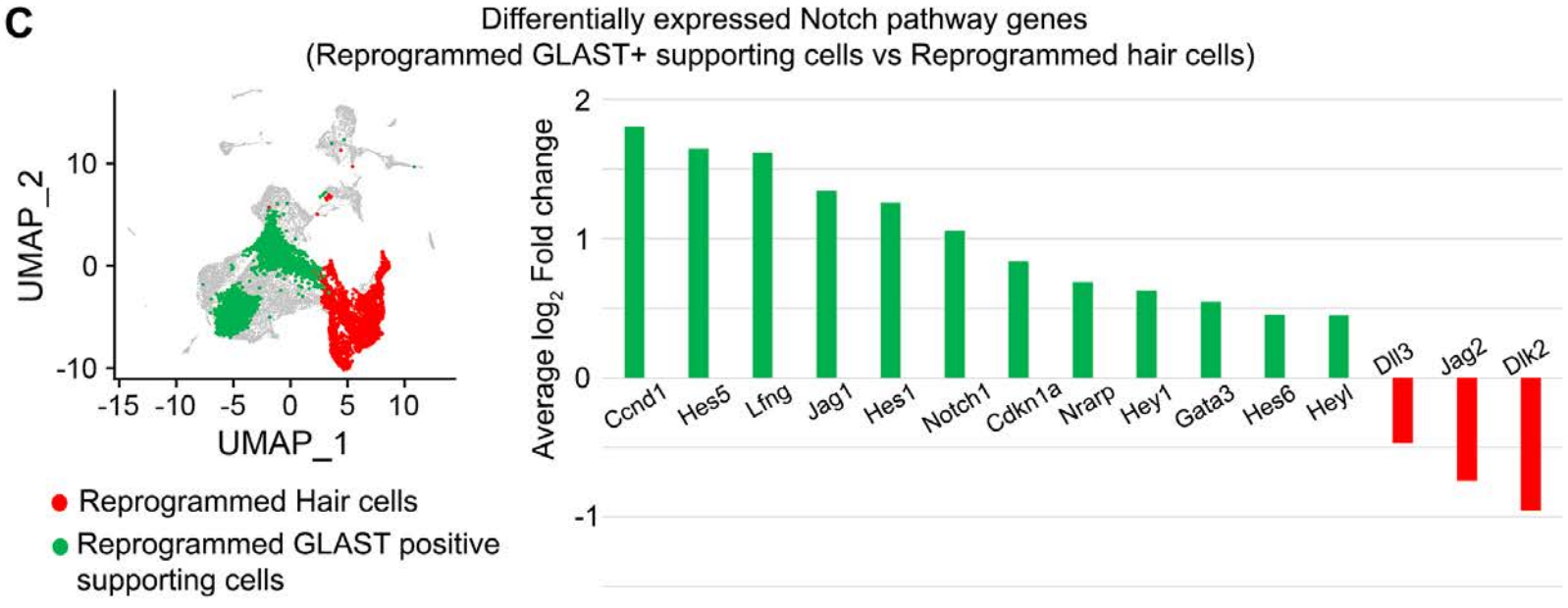

Pillar and Deiters cells do not get reprogrammed by P8 and P15 in response to transcription factor overexpression when targeted using the *Lfng-CreER* line

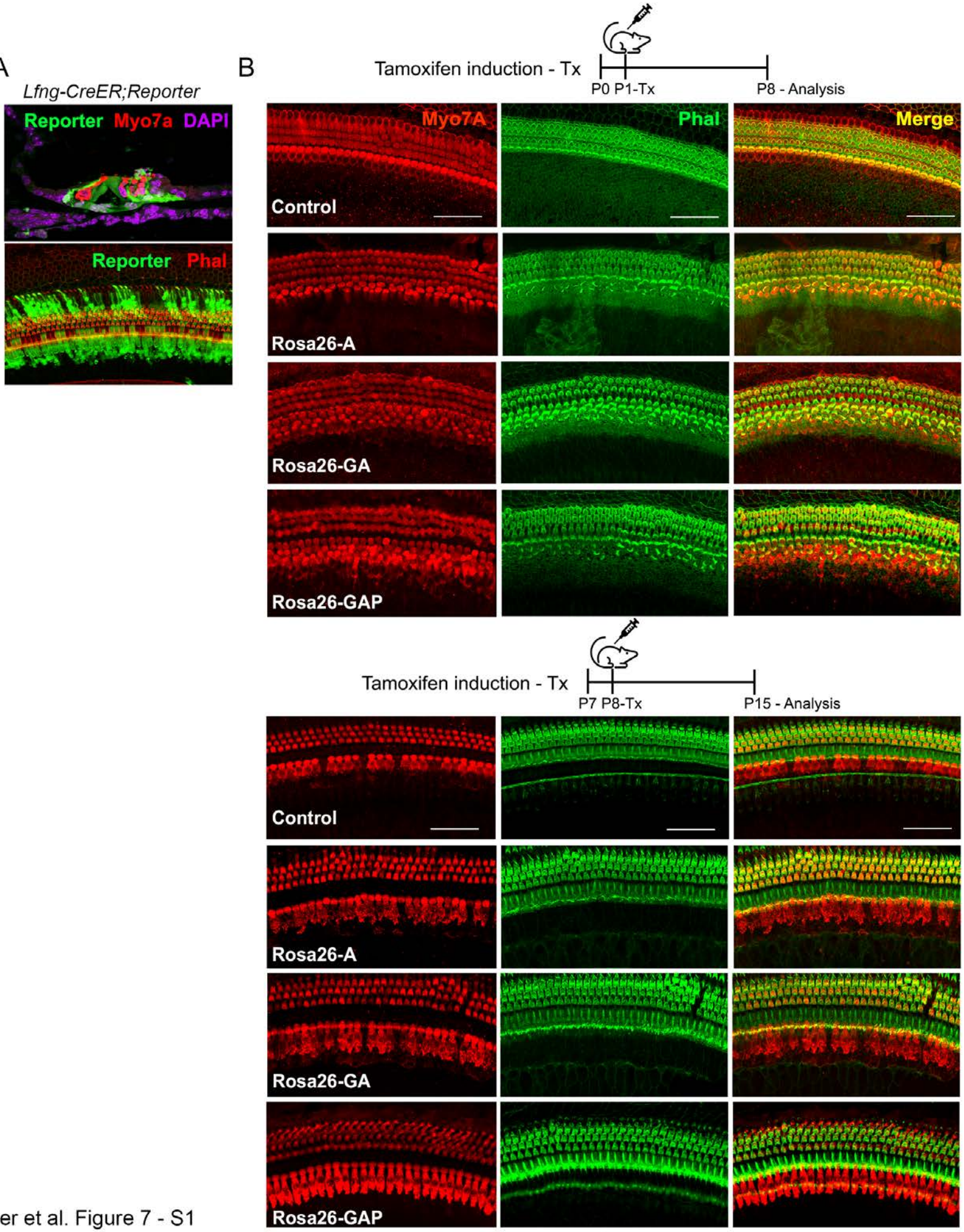

Iyer et al. Figure 7 - S1

A

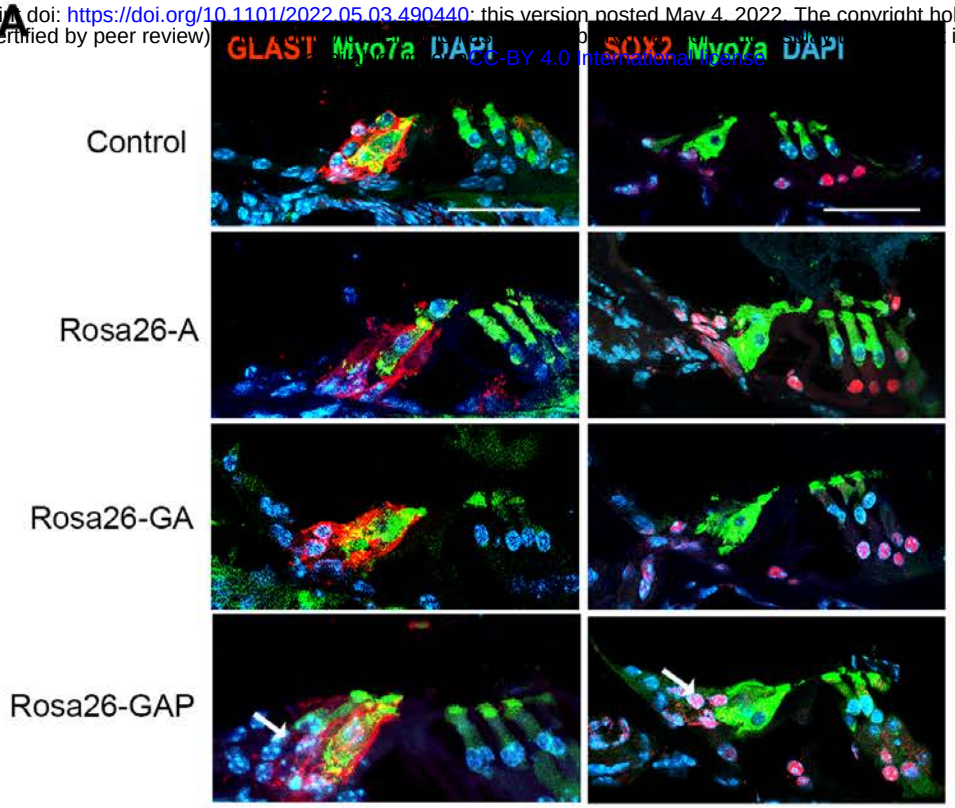

B

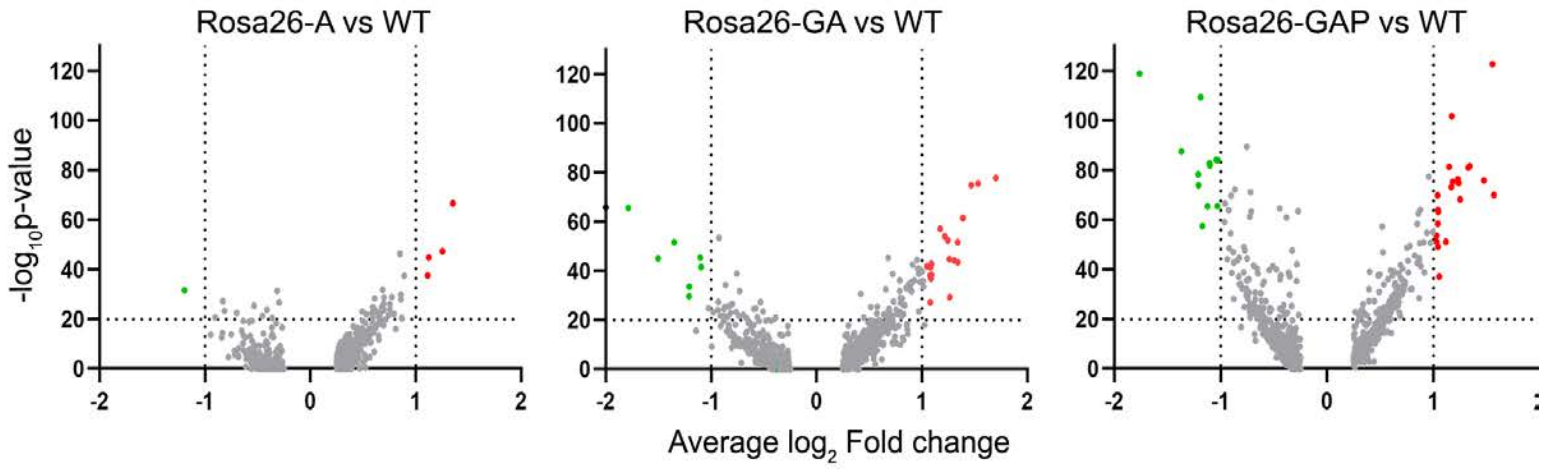

Down	Up
Ceacam16	*Cib2*
	Hes6
	Mdk
	Uchl1

Down	Up
Ceacam16	*Cib2*
Ttll3	*Agr3*
Rorb	*Col2a1*
Scd1	*Igfbp6*
Scnn1b	*Krt8*
Hhatl	*Mgst3*
Washc2	*Otoa*
	Slc5a3
	Tubb2b
	Fstl1
	Itga6
	Hes6
	Mdk
	Hes5
	Igfbp3
	Mfng
	Ccnd1
	Uchl1

Down	Up
Ceacam16	*Cib2*
Scd1	*Mgst3*
Rassf6	*Acbd7*
Ces1d	*Calml4*
Fibin	*Calb2*
Scnn1b	*Ccer2*
Kcnj16	*Lmo1*
Otol1	*Myl9*
Plcd4	*Tmem255b*
Hhatl	*Fabp5*
Washc2	*Gm266*
Hbb-bs	*Miat*
	Hes6
	Dlk2
	Ccnd1
	Mfng
	Mdk
	Hes5
	Igfbp3
	Uchl1

Supporting cell genes

Cochlear vasculature gene

Hair cell genes

Hair cell and non-hair cell genes implicated in the Notch and Wnt (*Uchl1*) signaling pathways

A. EdU labeling in the postnatal mouse cochlea

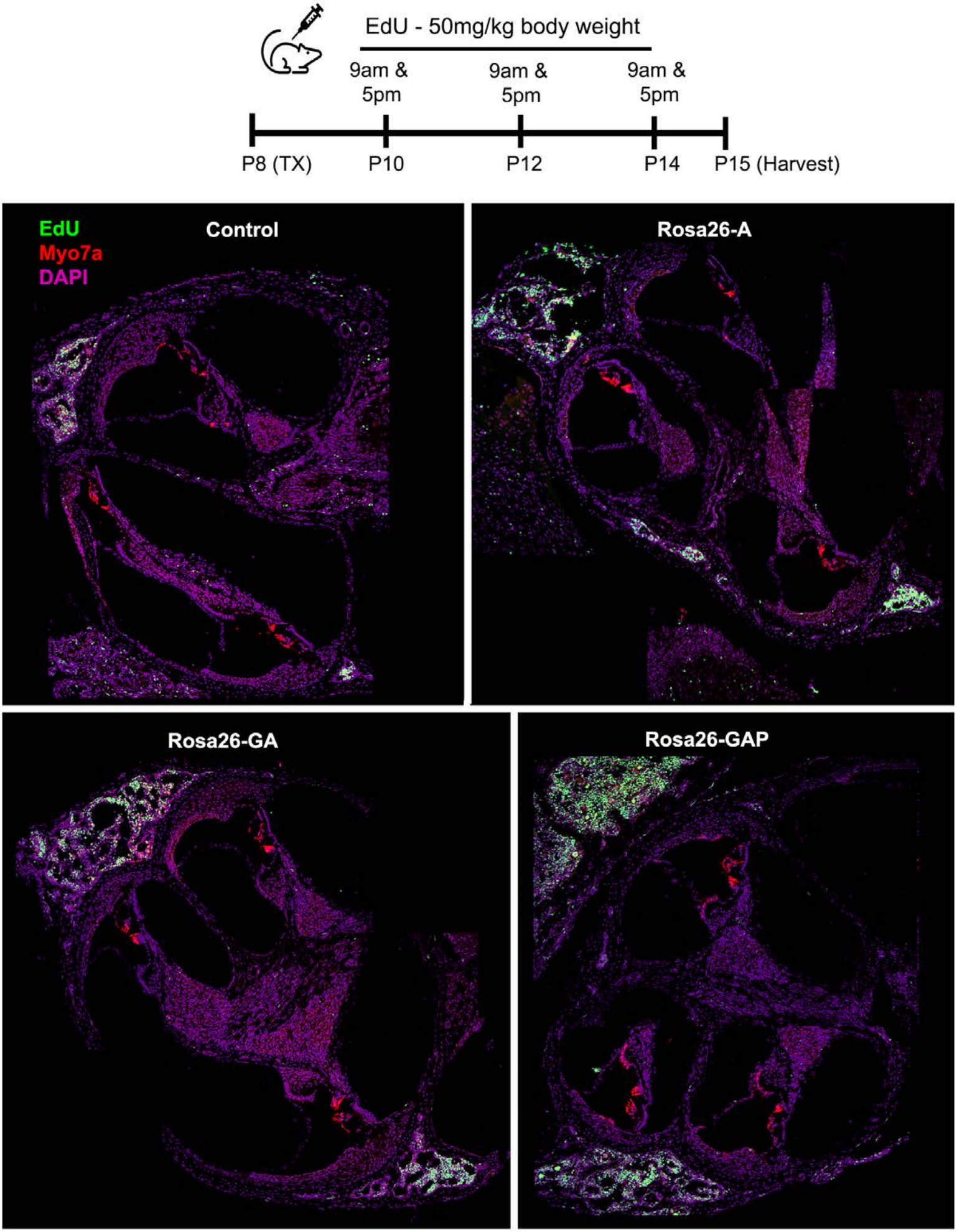

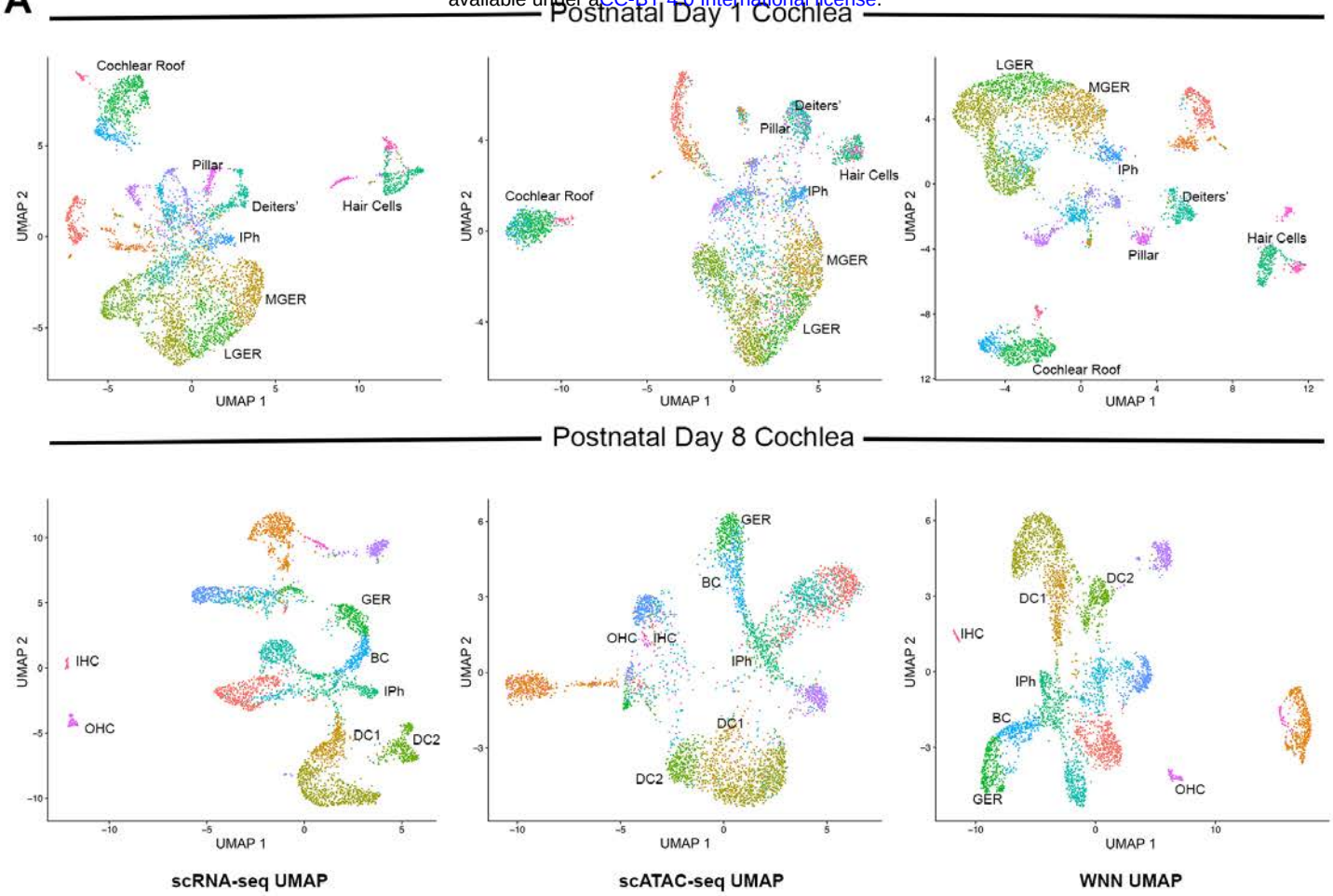

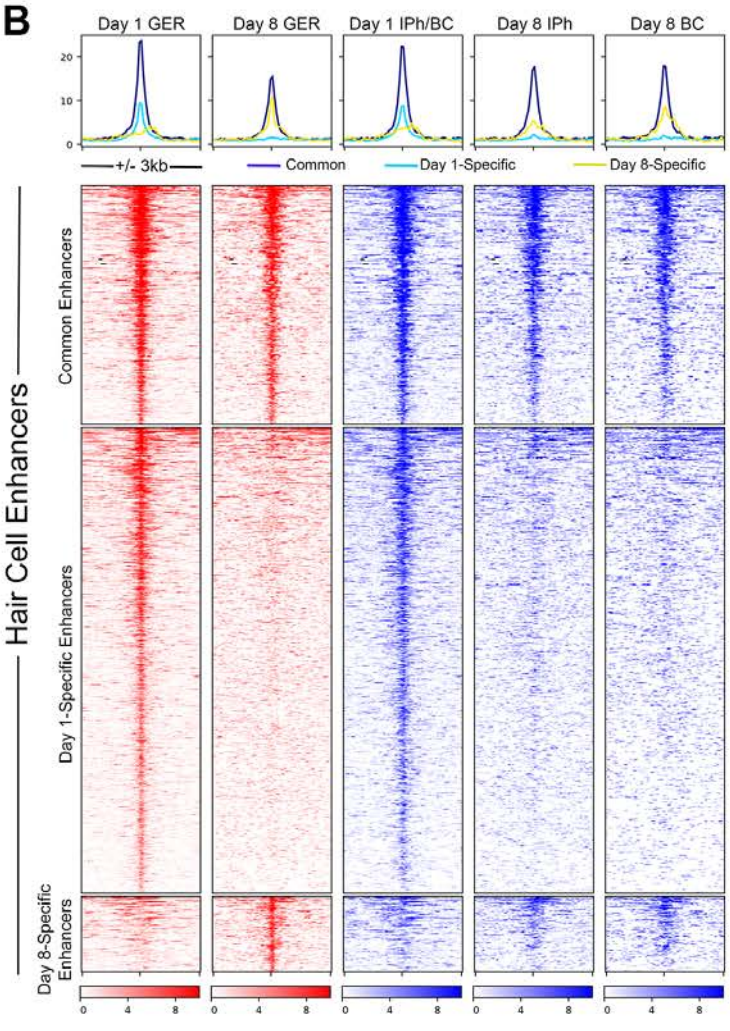

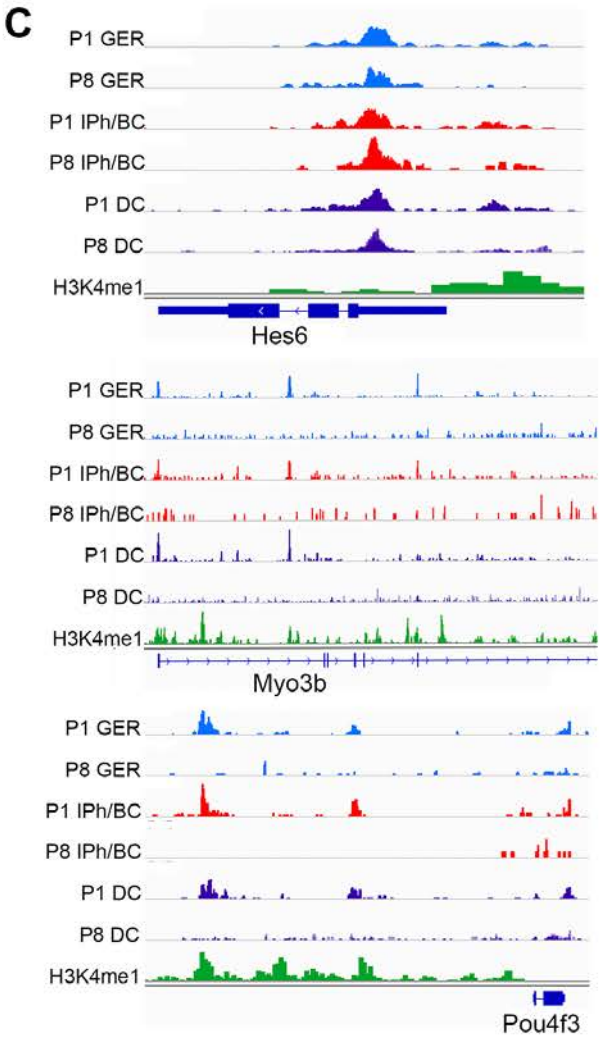

A. Endogenous *Pou4f3* expression three day after *Atoh1* induction

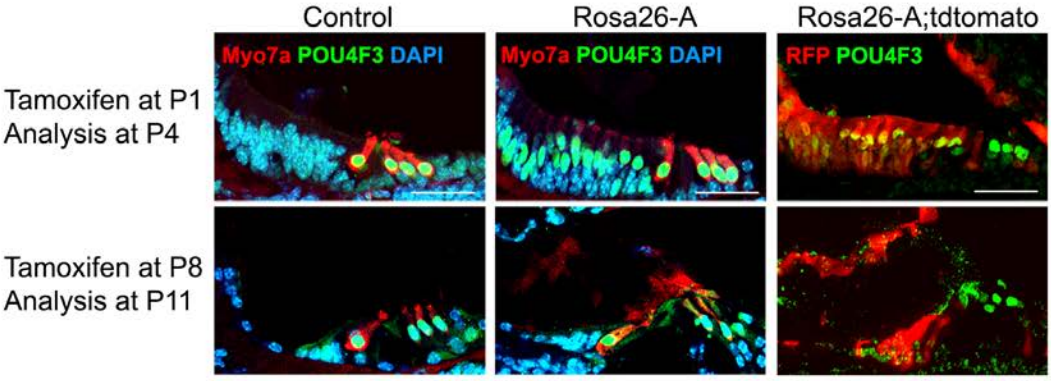

B. ATOH1 binding sites in the *Pou4f3* locus become less accessible with age

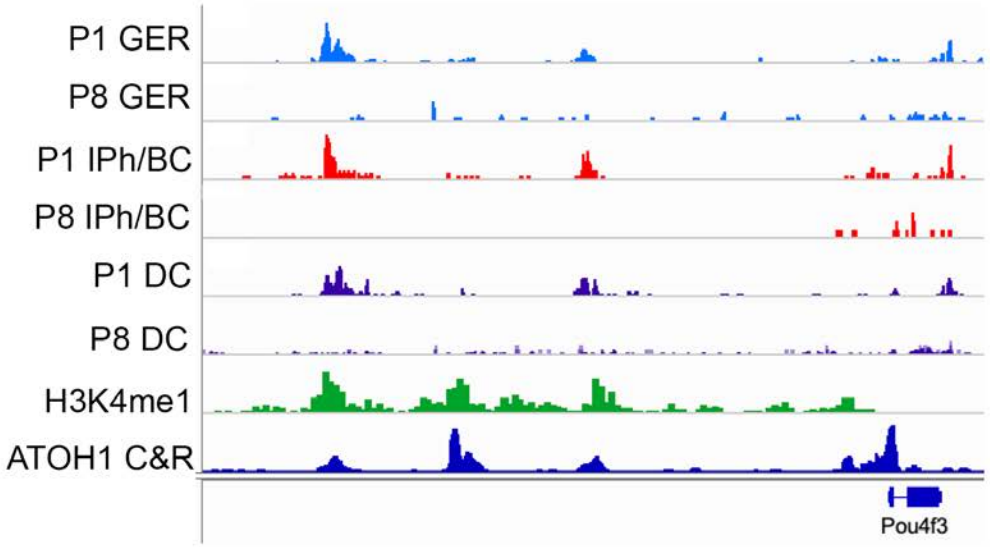

C. ATOH1 C&R E17.5 Hair Cells

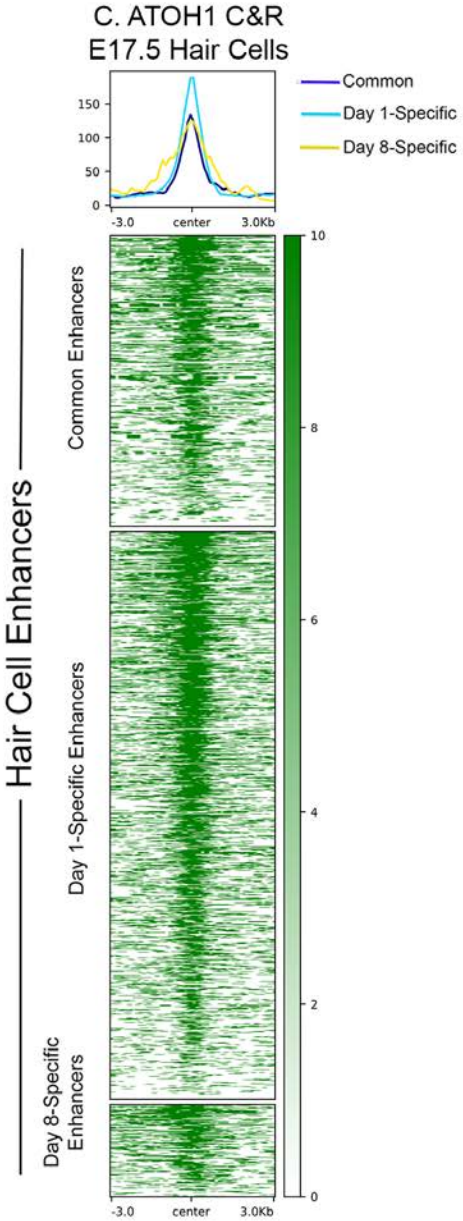

Iyer et al. Figure 9 - S1